

FRACTURE ANALYSES OF THE PALO DURO BASIN AREA,  
TEXAS PANHANDLE AND EASTERN NEW MEXICO

Edward W. Collins  
Barbara A. Luneau

Prepared for the  
U. S. Department of Energy  
Office of Nuclear Waste Isolation  
under contract no. DE-AC97-83WM46651

Bureau of Economic Geology  
W. L. Fisher, Director  
The University of Texas at Austin  
University Station, P. O. Box X  
Austin, Texas 78713

1985

**SUPERSEDED**

**DRAFT**

## CONTENTS

**Abstract**

**Introduction**

**Regional Fracture Patterns**

**Folds, Faults, and Joints**

**Fracture Identification Log Analysis**

**Field Investigations of Joints and Joint Spacing**

**Joint Spacing and Bed Thickness**

**Variability of Joint Orientations**

**Dissolution and Joint Density**

**Fractures and Veins in Core**

**Occurrence of Fractures and Veins**

**Gypsum Veins**

**Halite Veins**

**Anhydrite and Calcite Veins**

**Summary**

**SUPERSEDED**

**DRAFT**

## ABSTRACT

Fracture analyses of the Palo Duro Basin area, Texas Panhandle and Eastern New Mexico, provide clues to the structural history of the area and help to determine the occurrence and characteristics of the fractures and veins in strata of this region.

Fractures are associated with folds and faults that occur along the margins of the basin as well as in relatively undeformed strata within the central basin area. Along the Amarillo Uplift the strikes of fractures in Permian and Triassic rocks are different from fracture orientations in overlying Tertiary strata. Fracture orientations determined by fracture identification logs from wells in Deaf Smith and Swisher Counties indicate similar fracture strikes in Pennsylvanian and Permian strata within the basin. Throughout the region fractures that strike east-west ( $275^{\circ}$ - $295^{\circ}$ ) and northwest-southeast ( $305^{\circ}$ - $320^{\circ}$ ) are the most common. Zones of closely spaced fractures occur in outcropping Permian and Triassic strata. The width of the joint zones may be as great as 40 m and the zones may extend laterally for distances of up to 0.75 km or possibly farther.

Gypsum veins are common in strata that have undergone collapse following salt dissolution, whereas halite veins commonly cut salt-bearing strata. Even though a subpolygonal pattern on bedding planes suggests a synsedimentary origin for some of the halite veins, a variety of cross cutting relationships also indicate postcompactional origins for many of the halite veins.

## INTRODUCTION

Areas investigated in this study include the Palo Duro Basin and adjacent regions within the Texas Panhandle and eastern New Mexico (fig. 1). The stratigraphic section of this area is shown in figure 2. The Palo Duro Basin, an element of the late Paleozoic Ancestral Rocky Mountains structural system, is bordered on the north by the Amarillo Uplift, on the south by the Matador Arch, and on the west by the Sierra Grande Uplift and the Tucumcari Basin. These

**SUPERSEDED**

**DRAFT**

basement uplifts are fault controlled (Budnik, 1984). The Palo Duro Basin may have begun to form late in the Mississippian Period, and its development continued into the Permian Period (Totten, 1956). During basin development, uplifts bounding the basin were subaerially exposed, and coarse arkosic debris was transported into the basin (Dutton, 1980). After the Wolfcampian Epoch, the basin comprised marginal subtidal and supratidal marine evaporite environments, which existed throughout the rest of the Permian Period (Presley, 1981). Middle and Upper Permian evaporite deposits are composed of red mudstone, anhydrite, and bedded halite. The Permian section is overlain by rocks of the Triassic Dockum Group that were deposited in fluvial-deltaic and lacustrine systems (McGowen and others, 1979). Alluvial-fan sediments of the Neogene Ogallala Formation overlie the Triassic sediments (Seni, 1980).

Bedded Permian salt deposits of the Palo Duro Basin, Texas Panhandle, are being evaluated as potential sites for nuclear waste storage. Understanding the characteristics and densities of fractures in the rocks of the Palo Duro Basin is critical to geologic and hydrologic interpretations. Fractures influence the capability of rock to transmit and hold fluids. Fluid movement through fractures, and in particular closely-spaced fractures, may result in dissolution of evaporite strata (Goldstein and Collins, 1984; Gustavson and others, 1982). The purpose of this report is to define the regional fracture patterns of the Palo Duro Basin area, compare the fracture patterns of different age strata, and describe the characteristics of the fractures.

Fractures are any break in a rock due to mechanical failure by stress and include cracks, joints, and faults (Bates and Jackson, 1980, p. 244). Many of the fractures recognized in core during this study exhibit mineral fillings and are referred to as veins. Faults, joints, and veins have also been studied in outcrop.

Joints are fractures or partings in a rock that exhibit no displacement (Bates and Jackson, 1980, p. 334). Two styles of joints are systematic joints and nonsystematic joints (Hodgson, 1961). Systematic joints occur in sets. Joints composing each set are subparallel and are

**SUPERSEDED**  
2 **DRAFT**

commonly orthogonal to the upper and lower surfaces of the rock units in which they are present. Nonsystematic joints display no preferred orientation and commonly truncate against systematic joints.

Previous work on the origin and classification of fractures has determined several mechanisms to explain fracturing. Some researchers have explained fractures in terms of their relationship to tectonic deformation and major structural elements (Harris and others, 1960; Price, 1966; Stearns and Friedman, 1972; Nelson, 1979). Others have shown that fractures may develop independently from tectonic deformation and that joints may form in sedimentary rocks early in their history (Parker, 1942; Hodgson, 1961; Price 1966; Cook and Johnson, 1970; Nelson, 1979). Price (1974) characterized the development of fractures and stress systems in undeformed sediments during the accumulation of a sedimentary series, its downwarping and subsequent uplift, and accompanying dewatering of the sediments. Fractures can also result from unloading due to erosion (Chapman, 1958).

The study of systematic joints in outcrop within the Palo Duro Basin region has determined (1) the relationship between joint spacing and bed thickness, (2) the vertical and horizontal variability of joint orientations throughout the strata, and (3) the potential influence joint spacing might have on dissolution processes. Where outcrops do not exist, fracture identification logs (FIL) and core have been used to evaluate fracture orientations and the diagenetic and structural history of vein bearing strata.

#### REGIONAL FRACTURE PATTERNS

Regional fracture trends in the Texas Panhandle were determined by measuring joint strikes in outcrop and fracture orientations from fracture identification logs (FIL). Data for each one degree by one degree quadrant in the area has been plotted together. Outcrops are sparse in the Texas Panhandle; thus, there is a wide range in the number of measurements that were determined for the quadrants. The regional fracture trends are shown in figures 3a and

**SUPERSEDED DRAFT**

3c. Orientations that are statistically significant at a 95 percent confidence interval were determined using the chi-squared ( $\chi^2$ ) test of significance (figs. 3b and 3d). Methods for using this statistical test have been described by Dix and Jackson (1981).

A group of east-west oriented fractures with a mean azimuth range of 275°-295° occurs throughout the study area (figs. 3a and 3c) in both Permian and Triassic strata. Within the Permian strata, this set is statistically significant at a 95 percent confidence level in all but one quadrant (fig. 3b). Two northwest trending fracture groups also occur in the Permian rocks (fig. 3a). Their mean azimuth ranges are 305°-315° and 335°-350°. The group striking at 305°-320° occurs throughout the region and is also in Triassic rocks that crop out (figs. 3c and 3d). Fractures striking between 335°-350° are most common at the eastern part of the study area. Fractures also strike northeastward at 030°-060° (figs. 3a and 3c). These fractures prevail in the northwestern part of the study area and are not common southeast of Deaf Smith County (figs. 1, 3b and 3d). The least common fracture set, oriented at 000°-020°, is only observed in Triassic rocks (fig. 3d).

#### Faults, Folds, and Joints

Fracture orientations at various locations in the Texas Panhandle and eastern New Mexico coincide with trends of faults and folds. At the western margin of the Palo Duro Basin, joint trends are similar to the strikes of faults mapped from surface exposures (fig. 4a). The Bonita Fault and the Alamosa Creek Fault strike northeastward at 040°-050°. The Bonita Fault occurs in Quay County, New Mexico, and has been mapped and described by Lovelace (1972a, 1972b), Stearns (1972), Berkstresser and Mourant (1966), Dobrovolsky and others (1946), and Winchester (1933). The Bonita Fault is a normal fault that trends 040°-050°, dips 60° westward, and has a throw up to 700 feet. It is associated with an antithetic fault zone, so that the complete Bonita Fault System consists of a tilted graben block up to 1.5 miles wide. Cretaceous strata are faulted against Triassic Dockum rocks (Stearns, 1972). Tertiary Ogallala sediments appear to be folded at the southwestern part of the fault, whereas to the northeast,

**SUPERSEDED DRAFT**

Ogallala strata appear undisturbed. Shear and extension fractures are associated with the Bonita Fault Zone (Stearns, 1972).

In northern Roosevelt County the Alamosa Creek Fault has been mapped by Lovelace (1972b). The fault strikes at  $055^{\circ}$ ; the dip and throw have not been determined. The total faulted system comprises a graben block with Cretaceous strata faulted against Triassic Dockum strata, similar to the Bonita Fault System. Tertiary Ogallala sediments are folded and probably faulted.

The Bonita and Alamosa Creek structures are also recognized in the subsurface (fig. 4b). The structure (fig. 4b) exhibited at the base of the Permian San Andres Formation is below any salt dissolution that has occurred in this area. Boreholes drilled to basement are too sparse to determine the basement structure. Fractures associated with these faults may have influenced salt dissolution-collapse processes and possibly enhanced fault movement (Gustavson and others, 1980).

These faults strike similar to the northeast-southwest oriented regional fractures (fig. 3). Also aligned with these northeast trending structures is an unnamed fault located in Potter County, Texas, near latitude  $35^{\circ}30'$ , longitude  $101^{\circ}45'$  (fig. 5a). This small, normal fault strikes at  $045^{\circ}$  and dips  $80^{\circ}$ - $90^{\circ}$  to the southeast. The Permian Alibates Dolomite is offset 30 feet, and faulted Permian Quartermaster strata are overlain by undisturbed Tertiary Ogallala sediments.

Fractures also are associated with broad, drape folds related to dome-like structures of the Amarillo Uplift. East of the U.S. Highway 287 bridge crossing the Canadian River in Potter County, Texas, Permian, Triassic, and Tertiary strata gently dip  $0$ - $15^{\circ}$  south-southwestward off of John Ray Dome (figs. 5a and 5b). Triassic strata appear disconformable with overlying Tertiary Ogallala sediments. At several localities along the Canadian River, Ogallala sediments show an angular discordance with underlying Permian rocks; Triassic strata have been eroded away before or during Ogallala deposition. Also flanking John Ray Dome is a fault exposed at

**SUPERSEDED**

**DRAFT**

the surface that displaces Permian against Triassic rocks (Eifler, 1969). The strike of this fault is  $310^{\circ}$ - $295^{\circ}$ .

Along the southwestern flank of the John Ray Dome, joints in Permian Quartermaster, Triassic Dockum, and Tertiary Ogallala strata have been analyzed using azimuth versus traverse distance plots (AVTD) to detect any variability in the strike and the occurrence of joints along a traverse (Wise and McCrory, 1982). The locations of three traverses used for data collection are shown in figure 5b. The strike of a representative joint from each set was measured at intervals along each traverse. The joints are almost perpendicular to the sandstone beds; thus, even in the gently-dipping strata the joints are nearly vertical. Wise and McCrory (1982) describe the methods for plotting and contouring data for AVTD plots.

Joints in the Permian strata occur in two sets (figs. 6c and 6f). The predominant set strikes between  $300^{\circ}$ - $320^{\circ}$ . The AVTD plot (fig. 6c) shows this set is well defined. Other joints striking between  $050^{\circ}$ - $100^{\circ}$  are less common and appear irregularly along the traverse.

Two joint sets are also in the overlying Triassic sandstones (figs. 6b and 6e). Most of the joints strike between  $300^{\circ}$ - $320^{\circ}$ , and this set is well defined along the traverse (fig. 6b), similar to joints in the Permian rocks. These extension fractures parallel the drape fold axis and a nearby normal fault. Joints striking between  $030^{\circ}$ - $060^{\circ}$  are less abundant, and occur irregularly along the traverse (fig. 6b). The vertical joints in these strata are closely spaced. Sandstone beds 1 to 2 m thick commonly have 5-8 joints per meter.

Shear fractures with average dips of  $50^{\circ}$  are abundant in the Triassic rocks. Most of these fractures strike between  $295^{\circ}$ - $315^{\circ}$  and dip northeast and southwest (fig. 7a). Another group of fractures dip southeastward and strike between  $045^{\circ}$ - $065^{\circ}$ .

Orientations of joint sets and small-scale faults in basal, Tertiary Ogallala sandstones and conglomerates are different from those in Triassic rocks. Joint sets in the Ogallala rocks strike at  $020^{\circ}$ - $030^{\circ}$  and  $290^{\circ}$ - $300^{\circ}$  (figs. 6a and 6d). Both sets are well defined in the AVTD plot (fig. 6a). Normal faults with displacements less than 0.5 m also occur in the Ogallala strata. Two categories are based on the strike and dip of the faults: (1) faults that strike between

**SUPERSEDED**

**DRAFT**

260°-280° and dip nearly vertically and (2) faults that strike between 280°-300° and dip 50°-60° northeast and southwest (fig. 7b). Beds thicken on the downthrown blocks of several faults that dip 50°-60°. Faults and fractures are usually not common in Ogallala rocks elsewhere in the Texas Panhandle.

At the Triassic-Tertiary contact many of the northwest trending extension fractures in the Dockum sandstones are filled with fine-grained clastic material derived from the overlying Tertiary Ogallala Formation. Folding of the strata probably opened the fractures. Most of these clastic dikes are less than 1 cm thick and have a vertical length less than 2 m; however, the largest dike observed was traced vertically 13 m and is 10-15 cm thick.

The John Ray Dome is one of several regional anticlines associated with the Amarillo Uplift (Rogatz, 1939). Early studies by Powers (1922) identified only a few faults with small displacements associated with these domes. He attributed these domes to differential compaction of strata over basement highs rather than by recurrent motion of fault-bound basement blocks. However, basement fault motion should not be dismissed as a possible cause of the doming (Budnik, 1984). Extensive drilling throughout the region has identified more faults in the subsurface.

The variations between the fracture patterns in the Triassic and Tertiary rocks (fig. 7) suggest stress directions shifted after the deformation of the Triassic strata. The folding and fracturing of the Tertiary Ogallala rocks may be due to (1) stresses associated with regional deformation coincident with Basin and Range normal faulting to the west (Budnik, 1984) or possibly (2) stresses related to regional salt dissolution and subsidence (Gustavson and others, 1980).

Orientations of systematic joints in overlying undeformed strata of different ages may also vary. At the San Jon Hill area along the western Caprock Escarpment in Quay County, New Mexico, joints in Triassic, Jurassic, and Cretaceous strata were also studied using azimuth versus traverse distance plots (AVTD) (figs. 8 and 9). Joints striking west-northwestward between 270°-300° are predominant in all the strata. Joints that strike between 330°-360° are

**SUPERSEDED**

**DRAFT**

not common in the area, however they do occur irregularly in all the strata. Triassic and Jurassic strata also have northeast ( $050^{\circ}$ - $070^{\circ}$ ) striking joints. This joint group does not occur in overlying Cretaceous rocks, although joints striking between  $010^{\circ}$ - $030^{\circ}$  are present. In the Triassic strata gypsum veins fill only some of the northeast striking joints. Even though it is unknown what regional stresses may have affected strata in this area, some joint sets extend into overlying strata of different ages whereas other joint sets do not.

#### Fracture Identification Log Analysis

Schlumberger fracture identification logs (FIL) have been used to determine the orientation of vertical fractures in Pennsylvanian, Permian, Triassic, and Tertiary strata of Deaf Smith and Swisher Counties in the Texas High Plains where outcrops are sparse. During this study Permian evaporite beds in these counties were being evaluated for potential storage of radioactive wastes. The various uses and general description of FIL have been discussed by Brown (1978) and Beck and others (1977). In general, the geophysical tool consists of four pads 90 degrees apart, and when a pad crosses a fracture as the tool moves through the borehole, a change in resistivity is recorded. A curve representing changes in resistivity is recorded on the log for each pad. Permeable bedding planes are shown as thin spikes which correlate on all four curves, whereas vertical fractures are normally seen on only one or two pads. Vein-filled fractures or healed-fractures should only show a conductive anomaly if the vein material is more resistive than the surrounding rock. It is also likely that fractures (open or healed) occur in the direction of hole elongation at intervals of overbreak called breakouts (Babcock, 1978). Breakouts are recognized by separation of caliper curves on the FIL (fig. 10).

Accurate orientations of vertical fractures can be made if the fracture crosses two pads. Because the angle of hole deviation can affect accurate measurements, two logging units are available. On low-angle units the azimuth (to magnetic north) of pad 1 is recorded as the azimuth curve (azimuth of reference electrode), whereas for high-angle units the orientation of pad 1 is the addition of the azimuth curve (azimuth of hole deviation) and the relative bearing (Schlumberger, 1981).

<sup>8</sup>  
SUPERSEDED

DRAFT

Figure 10 shows a section of the FIL from the Stone & Webster-J. Friemel #1 borehole in Deaf Smith County (fig. 11). On the right side of the log are four columns exhibiting overlain curves for pads 1 and 2, 2 and 3, 3 and 4, and 4 and 1 (left to right). On the left side of the log are the hole deviation, relative bearing, and azimuth curves. A low-angle unit was used for this run, so the azimuth curve represents the azimuth of the reference electrode or pad 1. At a depth of 6,194-6,196 feet, curves for pad 1 and pad 3 show a change in resistivity that is interpreted as a fracture or zone of fractures. The azimuth of pad 1 is approximately  $270^{\circ}$ . With a magnetic declination near 10:E, the strike of the fracture crossing pads 1 and 3 is at  $280^{\circ}$ . At 6,215 feet a fracture is interpreted crossing pads 2 and 4. The azimuth of pad 1 is  $190^{\circ}$ ; thus the strike of the fracture (after correcting for magnetic declination) is at  $290^{\circ}$ .

FIL have been used to interpret fracture orientations in both cored and non-cored intervals of the boreholes in Deaf Smith and Swisher Counties. Core has been taken at selected depths for each test hole. Core observations recognized veins as well as fractures without mineral fillings. Fractures without mineral fillings have either a natural origin or have been induced by drilling/coring processes. These two styles of fractures have not been segregated in this study because the origin is not determinable for all the fractures. It is also possible that some mineral fillings may have been overlooked during the procedures of core description. Later in this paper the types of veins recognized in the core are discussed in detail.

FIL data from three boreholes in northeast Deaf Smith County (fig. 11) are plotted as frequency distributions (fig. 12). Data are sparse for Pennsylvanian strata; however, most of the fractures strike at  $300^{\circ}$ - $315^{\circ}$  and  $030^{\circ}$ - $040^{\circ}$  (fig. 12a). Two groups of fractures are also in Permian strata; they strike at  $030^{\circ}$ - $065^{\circ}$  and  $260^{\circ}$ - $315^{\circ}$  (fig. 12b). Several sets probably occur within these fracture groups. A set at  $270^{\circ}$ - $290^{\circ}$  is most common in Wolfcamp strata at the Stone & Webster-J. Friemel #1 borehole, whereas fractures in Permian strata at the other boreholes predominantly trend both west-northwestward ( $260^{\circ}$ - $315^{\circ}$ ) and northeastward ( $030^{\circ}$ - $065^{\circ}$ ). Orientations of fractures that occur in the cored intervals of Permian strata strike at  $280^{\circ}$ - $315^{\circ}$  and  $025^{\circ}$ - $040^{\circ}$  (figs. 12c and 13a). The strikes of veins and fractures with

**SUPERSEDED**

**DRAFT**

no mineral filling are almost the same (figs. 13b and 13c). In general, fractures in Pennsylvanian and Permian strata have similar strikes. Few fracture orientations were measured in Triassic and Tertiary strata (figs. 13d and 13e). Fracture orientations in Triassic and Tertiary strata are the same, however they differ slightly from the trends in the older strata (fig. 12). Data are too sparse to determine any significance from this observation.

In Swisher County data are from the Stone & Webster - Harman #1 and Zeeck #1 boreholes. Fractures in Pennsylvanian strata at the Zeeck #1 well, strike  $290^{\circ}$ - $310^{\circ}$  west-northwest (fig. 14a). The predominant fracture set in the Permian strata has the same trend (fig. 14b). This set ( $290^{\circ}$ - $310^{\circ}$ ) occurs at both borehole localities; however, the Stone & Webster-Harman #1 borehole also has a fracture set that strikes at  $020^{\circ}$ - $035^{\circ}$ . Fractures (all veins) in the cored Permian intervals strike at  $290^{\circ}$ - $300^{\circ}$  and  $020^{\circ}$ - $030^{\circ}$  (fig. 14c). Most of the joints measured at nearby outcrops of Triassic strata occur in two sets. They strike at  $280^{\circ}$ - $290^{\circ}$  and  $300^{\circ}$ - $320^{\circ}$  (fig. 14d).

This study indicates that fractures in Pennsylvanian and Permian strata within the Palo Duro Basin have similar fracture trends. Fractures in Triassic and Tertiary strata do not appear to strike the same as fractures in the older strata; however, data are sparse. Permian strata in both counties have a predominant fracture group striking west-northwest at  $260^{\circ}$ - $315^{\circ}$ ; several sets probably occur within this group. Northeast ( $030^{\circ}$ - $065^{\circ}$ ) trending fractures appear to be more common in Deaf Smith County than Swisher County. The fracture orientations interpreted from FIL correspond with the regional fracture patterns recognized in the area (fig. 3).

#### FIELD INVESTIGATIONS OF JOINTS AND JOINT SPACING

Field studies on systematic joints in Permian and Triassic strata were conducted at Caprock Canyons and Palo Duro Canyon State Parks in Briscoe and Randall Counties, respectively. They indicate that: (1) zones of closely spaced joints are common, (2) joint

**SUPERSEDED**

**DRAFT**

spacing varies with bed thickness, and (3) joint sets may occur either constantly, randomly or display systematic variations in strike. Joints and joint spacing also may significantly influence dissolution processes.

### Joint Zones

Zones of closely-spaced joints (joint zones) exist throughout Permian and Triassic strata in both Cap Rock Canyons and Palo Duro Canyon state parks. Figure 15 shows a joint zone drawn from a photograph-mosaic. The zones studied range in width from 10 to 40 m and may extend laterally for distances of up to 0.75 km or possibly farther. The actual spacing of joints within these zones cannot be accurately measured from photograph-mosaics because not all of the joints are visible. Joint zones in the areas studied extend vertically through Permian and Triassic beds, but there is no evidence that the zones cut the Tertiary Ogallala Formation. This may be partially a result of poor exposures and the coarseness and composition of the unit. The Ogallala Formation is composed of sand, silt, clay, gravel, and caliche, and is cemented locally with calcite and silica.

### Joint Spacing and Bed Thickness

Bed thickness affects the spacing of the joints within and beyond zones of closely spaced joints. At the two state parks, the number of systematic joints across two meter lines (joint density) were measured for sandstone and siltstone beds of different thicknesses. The joint density data are numerically weighted and the joint density mean values are plotted with the log of the bed thickness in figure 16. Data within zones of closely spaced joints (joint zones) are plotted separately.

The two curves comprised of data from Caprock Canyons and Palo Duro Canyon show joint density values drop from 20 and 12 joints per 2 m to 5 joints per 2 m when bed thickness increases from 0.06 m to 0.5 m. For a bed thickness of 1.0 m the mean joint density is 3 to 4 joints per 2 m, and as bed thickness nears 3.0 m the mean joint density is 3 joints per 2 m.

SUPERSEDED  
11

**DRAFT**

The joint density vs. bed thickness curve for data of joint zones (fig. 16) has a similar shape as the curves for Caprock Canyons and Palo Duro Canyon data, although greater joint density values are expressed. In joint zones, mean joint density values are 10 to 9 for beds 0.5 m to 3.0 m thick. The curve shows joint densities increase substantially for bed thickness values less than 0.3 m.

#### Variability of Joint Orientations

Orientations of gypsum-filled vertical joints were studied at Palo Duro Canyon State Park. AVTD techniques (Wise and McCrory, 1982) that were discussed previously in this paper were used for this study. Strikes of vertical gypsum veins in Permian strata were measured along three traverses at the canyon (fig. 17). The strikes of the mineral-filled joints are displayed by AVTD plots and rose diagrams in figure 18. The gypsum fill in the joints was probably derived from evaporite dissolution (Goldstein and Collins, 1984); thus these joints predate slump features associated with more recent unloading processes and canyon development.

Veins striking east-west ( $070^{\circ}$ - $100^{\circ}$ ) are common throughout the area. These mineral-filled joints are well defined in the AVTD plots (fig. 18) although they do not represent the most common joint trend in the area. Most of the mineral-filled joints strike northwest-southeast, similar to the overall canyon orientation. The AVTD plot for traverse 1 shows most of the joints striking north-northwest at  $340^{\circ}$ - $360^{\circ}$ . This joint trend is common in the plot for traverse 2, however southward along this traverse, the strikes of the north-northwest trending joints drift from  $340^{\circ}$ - $360^{\circ}$  to  $320^{\circ}$ - $340^{\circ}$ . Along the southern segment of traverse 2 joints with north-northwest ( $320^{\circ}$ - $340^{\circ}$ ) strikes are absent, but joints that strike  $300^{\circ}$ - $320^{\circ}$  are common. Joints striking  $300^{\circ}$ - $320^{\circ}$  are also most abundant along traverse 3.

The AVTD plots show that where joints oriented between  $320^{\circ}$ - $360^{\circ}$  are most abundant, joints striking  $300^{\circ}$ - $320^{\circ}$  occur irregularly; conversely, where most joints strike  $300^{\circ}$ - $320^{\circ}$  the

**SUPERSEDED**

north-northwest ( $320^{\circ}$ - $360^{\circ}$ ) and northeast-southwest striking joints are not abundant. Joints that strike east-west ( $070^{\circ}$ - $100^{\circ}$ ) are common throughout the area.

**SUPERSEDED** 13

**DRAFT**

## Dissolution and Joint Density

Geologic investigations show that dissolution of Permian rocks has occurred and is occurring in the Texas Panhandle and eastern New Mexico (Bachman, 1980; Gustavson and others, 1980; Gustavson and others, 1982; Simpkins and others, 1981). Local dissolution near the surface in the vadose zone develops sinkholes and caves. Regional dissolution in the vadose or phreatic zone develops caves and solution breccias. Deep-seated dissolution can be generated in the phreatic zone, forming deeper caverns. These types of dissolution in gypsum, anhydrite, and halite are dependent on fractures that allow movement of fresh water to soluble rocks (Bachman, 1980).

Evidence derived from several outcrops at Palo Duro Canyon State Park, Randall and Armstrong Counties, and Caprock Canyons State Park, Briscoe County, suggests that joints and joint density are important to dissolution and erosion processes. Erosion by running water forms caves in sandstone where greater-than-average joint densities occur. The cave shown in figure 19 has formed where the joint density is 10 joints per 2 meters. Away from the cave entrance the joint density is 4 joints per 2 meters. Figure 20 shows where fractures in gypsum are enlarged, and hollows or small caves commonly have developed due to dissolution along joints.

Dissolution cavities along fractures in gypsum beds were studied to determine the effects of joint density on dissolution processes. Figure 21 compares joint density values with cavity percentages across 2 m lines, and indicates cavity space increases with greater joint density values. A linear relationship is expressed in figure 21 and the correlation coefficient of 0.97 indicates a good relationship among the data. These data indicate that close spacing of fractures may create a greater potential for dissolution by fluids.

14  
**SUPERSEDED**

**DRAFT**

## FRACTURES AND VEINS IN CORE

Permian strata of the Texas Panhandle are cut by gypsum, halite, anhydrite, and calcite veins, as well as fractures with no mineral filling. Fractures without mineral fillings are either natural or induced by the drilling/coring procedures. It is also possible that some mineral fillings may have been "washed-out" during core retrieval and preparation, or that the fillings may have been overlooked during description of the core. Halite veins are common in the halite-bearing strata of the San Andres, Glorieta, upper Clear Fork, Tubb, lower Clear Fork and Red Cave Formations (fig. 2). Overlying the salt-bearing units are strata that exhibit evidence of halite dissolution. These strata include the Dewey Lake, Alibates, Salado-Tansill, Yates and Seven Rivers Formations (fig. 2). Gypsum veins are abundant in these units. In Wichita and Wolfcamp strata that underlie the halite-bearing formations calcite- and anhydrite-filled fractures are present. Fractures without mineral fillings also occur in these strata.

### Occurrence of Fractures and Veins

The abundance of fractures (including veins) in Permian strata has been analyzed in core from boreholes drilled in Oldham, Deaf Smith, and Swisher Counties (fig. 11). The cored strata range from Wolfcamp Group to the Alibates Formation. Units are grouped into three categories based on lithology and stratigraphic sequence (Hovorka, personal communication, 1983). The categories are (1) strata below salt units (Wolfcamp Group), (2) salt zone units, and (3) dissolution zone units. The boundary between the dissolution zone units and the salt zone units is not the same at each borehole.

The number of one-foot intervals that contain fractures (veins and non-filled fractures) are recorded for all of the cored intervals. Fractures that have been interpreted as the result of drilling/coring procedures have not been recorded. However, the origin for many of the non-filled fractures recognized in the core is unknown and some may be due to the drilling/coring operations. Guidelines to recognize natural and drilling induced fractures have been described

by Kulander and others (1979) and Sangree (1969). The percentage of fractured core for each unit is determined by dividing the number of one-foot core intervals containing fractures by the total core footage and then multiplying by one hundred.

Figure 22 compares the boreholes and the percentage of fractures and veins in the core for the units (1) below the salt zone, (2) within the salt zone, and (3) within the dissolution zone. The dissolution zone units are more fractured than salt zone units. The salt zone unit category contains the lowest percentages of fractured core, probably because the fractures or veins almost always occur in thin mudstone, siltstone, and anhydrite interbeds. Veins within the thicker salt sequences are rare. The DOE-Stone & Webster #1 Mansfield borehole in Oldham County has the greatest percentage of fractured core for the Wolfcamp category. This might be expected, because this borehole is located within the Bravo Dome-Amarillo Uplift area. The uplift area borders the Palo Duro Basin on the north and is believed to have been more tectonically active than the basin during and after Permian time. The frequency of fractures in Wolfcamp core decreases away from the Bravo Dome-Amarillo Uplift. The fracture and vein percentages in core within the salt zone units are similar for all boreholes in the three counties.

The fractures are commonly filled with gypsum, halite, anhydrite, or calcite, and stratigraphic intervals are characterized by distinct vein compositions. Vein fillings within the salt dissolution zone strata are predominantly fibrous gypsum (fig. 23).

Veins within the salt zone units are characterized by fibrous halite, commonly 0.5-1.0 cm wide. The veins usually occur within mudstone, siltstone, and anhydrite beds. Halite fills more than 80 percent of the fractures in the salt zone strata (fig. 24).

In the strata beneath the salt zone units, the fractures are commonly filled with anhydrite and calcite or have no vein fillings (fig. 25). Halite veins also occur within upper Red Cave strata in the Oldham County, DOE-Stone & Webster #1 Mansfield borehole. The veins in the units beneath the salt-bearing strata are usually less than 1.0 cm wide.

## Gypsum Veins

Gypsum veins in the Palo Duro Basin are associated with units exhibiting evidence of halite dissolution and have been extensively studied in field exposures by Goldstein (1982) and Goldstein and Collins (1984). Veins in vertical, horizontal and inclined orientations are filled with antitaxial fibrous gypsum (Ramsay and Huber, 1983) and commonly have a medial suture line. The same general relationship is recognized for gypsum veins present in the core (fig. 26). Veins in core were studied in the DOE-Stone and Webster #1 Rex White, #1 Mansfield, #1 J. Friemel, #1 Harman, #1 G. Friemel, and #1 Woods-Holtzclaw wells. Thin sections of veins were studied in the DOE-Stone & Webster #1 Rex White and #1 Mansfield boreholes.

Horizontal and obliquely oriented veins are most commonly observed in the core. The veins occur primarily in the clastic Alibates, Salado-Tansill, Yates, and Seven Rivers Formations. Vein thickness ranges from 1 mm to 5 cm. The veins consist of fibers about 1 mm in diameter oriented perpendicular to the walls in most cases. There may or may not be a medial suture present in the central portion of the vein. When present, the medial suture may be marked by fragments of siliciclastic wall material or interlocking gypsum crystals. In thin section, the suture is marked by a linear zone of more finely crystalline gypsum (fig. 27). Some of the thicker veins have sigmoidal-shaped fibers across the width of the vein indicating simple shear during the filling stages.

Oblique veins tend to be linear and have straight, sharp wall contacts. Horizontally oriented veins display straight, linear contacts and contacts of a more irregular nature. Veins which have irregular wall contacts tend to be thinner (less than 1 cm) and less continuous than the straight-walled veins. These veins have an anastomosing appearance with protruding fingers (fig. 28). The host for the more irregularly shaped veins is most commonly intraclastic mudstone or siltstone with gypsum, dolomite, and anhydrite rimming the clasts. This fabric has been interpreted as a dissolution residue (Hovorka, in press). Uniform and continuous, straight-walled veins are present in ripple-laminated and mildly contorted red/brown siltstone and mudstone.

17

**DRAFT**

In the dolostone and gypsum/anhydrite of the Alibates Formation, veins are present along stylolite surfaces. Vein walls are irregular on a small scale, and there is a dark-colored residue along the walls. The gypsum veins also transect stylolites.

Irregularly-shaped veins fill nonsystematic fractures. Veins with straight-walled contacts fill systematic joints and bedding planes. There is a close association of dissolution textures and the occurrence of gypsum veins in the cored strata. Gypsum veins with extension fibers are believed to result from the dissolution of evaporites and collapse of the overlying strata (Goldstein and Collins, 1984).

#### Halite Veins

Fibrous halite veins in the San Andres, Glorieta, upper Clear Fork, Tubb, lower Clear Fork, and Red Cave strata (halite-bearing interval) were studied in core from the DOE-Stone & Webster #1 Mansfield, #1 Harman, #1 J. Friemel and the DOE-Gruy Federal #1 Rex White boreholes. Veins are present in normal marine mudstone and carbonate units, base-of-cycle mudstones, terrestrial siliciclastics, and mudstone and siltstone interbeds of bedded and recrystallized halite units. Halite veins are not observed in the anhydrite units; they are observed in anhydrite nodule-rich carbonate units but pinch out upwards as anhydrite density increases. In carbonate units overlain by anhydrite, veins pinch out below or abut against the anhydrite bed.

Most halite veins are deep red-orange in color. Chemical analyses to identify pigments have not been completed, but in similar occurrences in Devonian Salt near Elk Point, Alberta (Wardlaw and Watson, 1966) and the Hutchinson Salt, Kansas (Dellwig, 1968), the color is due to ferric iron. Microprobe analysis has failed to reveal polyhalite which indicates that the color is not due to its presence. Colorless and color-zoned fibrous veins also exist.

Halite in all veins has a fibrous texture. Narrow veins are composed of single fibers (1 mm in diameter) across the width of the vein oriented perpendicular to the walls (fig. 29). Veins wider than 2 cm commonly show multiple sigmoidal-shaped fibers across the width of the vein (fig. 30).

SUPERSEDED  
18

**DRAFT**

Most fractures are straight walled and vertically oriented. They are elliptical in shape and pinch out at both ends resembling tension gashes (fig. 31). Most veins are less than 1 cm wide. In the upper and lower Clear Fork and Tubb Formations of the #1 Mansfield well, some veins are at least as wide as the core (10 cm) and more than one meter long. Where veins occur in thin mudstone and siltstone interbeds in halite, the length of the veins is limited by the thickness of the interbed. Vein length is variable in the basal mudstones and carbonates.

The interpretation of the timing of fractures is difficult; evidence supports both a synsedimentary and a postcompactional origin. Halite-filling fractures between salt polygons formed by syneresis or desiccation in the sedimentary environment are widely recognized in modern and ancient evaporites (Hunt and others, 1966; Dellwig, 1968; Tucker, 1981; Handford, 1982). In the Palo Duro Basin, a subpolygonal pattern is recognized on bedding planes for a few cases of small, intersecting veins in thin mudstone interbeds in halite units. Desiccation or thermal contraction in a subaerial flat environment is a possible origin for these veins.

Examples of crosscutting relationships show that many veins postdate compaction and cementation. A halite vein in carbonate grainstone of the upper San Andres Formation, #1 Mansfield well, cuts across ooids, fracturing individual grains as opposed to breaking around the ooids (fig. 32) suggesting that fracturing occurred following lithification. Veins present in microstylolitized carbonate of the upper Clear Fork Formation, #1 Mansfield well, indicate fracturing following compaction and show no disturbance of laminae at vein walls (fig. 33). The presence of veins in normal marine carbonates and base of cycle mudstones indicate brines penetrated buried sediments. A lack of pygmatic features that have been described as being associated with precompactional structures in other areas (Van Houten, 1964; Spencer and Spencer, 1972) is further evidence of a postcompactional origin. Additionally, the veins parallel the trends of regional fracture patterns, suggesting that the development of the fractures was influenced by regional stresses (figs. 1 and 2).

Geochemical and diagenetic evidence supports an early origin for fractures. Some anhydrite nodules in both mudstone and carbonate formed before fracturing and are fractured

19  
SUPERSEDED

DRAFT

flush with the vein walls. In other cases, anhydrite nodules protrude into the vein or are completely healed across the vein (fig. 33) indicating that anhydrite as well as halite was available in the geochemical environment during vein formation. Much of the anhydrite diagenesis is thought to have been active during the early diagenetic history as indicated by extensive anhydrite replacement of gypsum and pseudomorphic textures (Hovorka, 1983).

Silica and multi-faceted dolomite are other diagenetic phases associated with the halite veins. Dolomite and silica are present in minor amounts along fiber crystal boundaries. Silica and dolomite are also observed as the common diagenetic phase in halite in mud elsewhere in the evaporite section (Hovorka, 1983). This suggests that the veins do not represent a separate (later or earlier) diagenetic event.

Geochemical analyses of bromide concentrations were done to determine differences between vein salt and other forms of halite, such as bedded and recrystallized salt. In an open system, the bromide concentration in halite at successive stages of crystallization changes as a result of partitioning. The first halite to crystallize from seawater commonly has bromide concentrations on the order of 75 ppm. Lower bromide concentrations have been considered evidence for dissolution and secondary deposition of halite, and higher bromide concentrations suggests greater levels of salinity at the time of crystallization (Holser and others, 1972; Holdoway, 1978). Figure 34a illustrates the distribution of bromide values for the upper Clear Fork, Tubb, and lower Clear Fork veins and other salt. The values for the veins fall within the distribution for other salt; though they are skewed, the values are not significantly different. The similarity in bromide values for vein halite in both the bedded and recrystallized halite units suggests that the veins were derived from the same or similar brines that deposited the bedded and recrystallized halite. A substantial difference in bromide values would represent a separate brine resulting from more advanced evaporation or later dissolution (Holser and others, 1972). Similar relationships are noted for veins and other salt in the upper and lower San Andres formations (figs. 34b and c).

SUPERSEDED  
20

**DRAFT**

Several characteristics indicate that the major veins present in the extensive siliciclastic units of the Clear Fork and Tubb Formations, base of the cycle mudstones, and normal marine carbonates are not desiccation or dissolution features. The following observations argue against a desiccation origin: 1) the fibrous texture suggests that the fractures opened under the influence of a stress field; 2) the veins do not exclusively "V" downwards; they are elliptical in shape; 3) the fracture filling is not zoned and contains no silt or mud infilling. The predominance of vertical orientations and lack of inclined and horizontal halite vein orientations does not support a dissolution origin. Furthermore, there is limited evidence of late stage regional dissolution in the underlying units.

The factors thought to be important in interpreting the history of the halite veins are as follows. Small veins present in mudstone and siltstone interbedded with bedded halite units exhibiting a subpolygonal pattern on bedding planes may have a desiccation or synaeresis related origin. Major veins present elsewhere in the section (base of cycle mudstones, normal marine carbonates, extensive siliciclastic units) exhibit a postcompactional origin as indicated by the above described crosscutting relationships. The similarity in diagenetic numerals in the veins to halite elsewhere in the section suggest that the veins do not represent a unique diagenetic event in themselves. The similarity in bromide values between the veins and other halite supports crystallization from similar brines. The consistency of orientation parallel to regional structural trends suggests that fracture opening was influenced by the regional stress system. Halite veins in the Palo Duro Basin are not a unique occurrence; the presence of similar veins in other basins (Devonian of Alberta, Hutchinson Salt of Kansas) suggests that similar factors may have been operative in the development of halite veins in evaporite environments elsewhere.

The timing of halite vein emplacement in the evaporite section of the Palo Duro Basin is thought to be postcompactional, but early enough to be associated with shallow diagenetic phenomena. Emplacement most likely occurred in an environment removed from the surface but which continued to be influenced by the overlying regime of evaporite deposition.

## Anhydrite and Calcite Veins

Few veins are observed in the Wichita and Wolfcamp strata underlying the salt-bearing units of the Palo Duro Basin. Veins are most commonly observed in the DOE-Stone & Webster #1 Mansfield well which flanks the Bravo Dome-Amarillo Uplift. Veins of calcite or anhydrite are sporadically distributed and are commonly 1 to 3 cm in length. They are usually less than 3 mm wide. These veins are composed of crystalline mosaic calcite and anhydrite. Some veins appear to be associated with anhydrite nodules and zones of differential cementation. Others transect well cemented wackestone and packstone. The origin of these veins is unknown.

### SUMMARY

Fractures in Pennsylvanian and Permian strata of the Palo Duro Basin area were probably formed by stressed systems associated with the development of the basin and the surrounding areas of uplift. On an outcrop scale, strikes of joints in Tertiary Ogallala strata exposed along the Canadian River Valley in Potter County differ from joint orientations of underlying Triassic and Permian rocks suggesting a different stress field affected the Tertiary strata. Regionally, fractures have both similar and differing orientations in Permian and Triassic strata. Fractures in Tertiary Ogallala strata are not common regionally.

Fractures are associated with folds and faults that occur along the margins of the Palo Duro Basin and joints also occur in undeformed strata within the basin. Joints in relatively undeformed sediments probably were formed by stress systems that were active during accumulation, compaction, and downwarping of the sediments, and subsequent uplift of the sedimentary series. In Permian and Triassic rocks that crop out in the area, east-west ( $275^{\circ}$ - $295^{\circ}$ ) and northwest-southeast ( $303^{\circ}$ - $320^{\circ}$ ) oriented fractures are common. Northeast ( $030^{\circ}$ - $060^{\circ}$ ) striking fractures are most abundant in the western part of the study area. In situ stress measurements determined from hydraulic fracturing of Permian strata in the Stone and Webster #1 Holtzclaw well indicate that regional principal compressive stress is northeast-southwest

22

**DRAFT**

(Gustavson and Budnik, 1985). Unfilled fractures that are parallel to the in situ principal compressive stress are the most likely to serve as fluid conduits.

Zones of closely-spaced fractures were recognized in Permian and Triassic strata that crop out along the eastern Caprock Escarpment. These zones are 10 to 40 meters wide and locally extend laterally for at least 0.75 km. The density of joints in these zones is about 10 joints per 2 m for beds 0.5 to 3.0 m thick. Away from the joint zones joint densities are 5 joints per 2 m for beds 0.5 m thick. The spacing of joints has the potential to influence dissolution processes. Where joint density is greater, dissolution is potentially more extensive.

Gypsum, halite, and calcite veins are common in core of Palo Duro Basin Permian rocks. The dissolution units, the halite-bearing units, and the strata below the halite-bearing units are each characterized by a unique suite of veins and fractures. Fibrous gypsum veins are present in the units having undergone dissolution. Veins of white gypsum are on the average of 1 to 1.5 cm wide and characterized by a medial suture line. Oblique, horizontal, and vertical orientations are common. The veins developed in response to late-stage regional dissolution of underlying evaporite units.

Red, fibrous halite veins are common in siliciclastic, carbonate, and base of cycle mudstone units of the salt-bearing formations. The veins are primarily vertically oriented and elliptical in shape. Vein width averages about 1 cm but ranges to as wide as 10 cm, vein length is also variable and veins as long as 1 m have been recognized. There is evidence for syn-sedimentary and postcompactional origins. Cross-cutting relationships, diagenetic and geochemical evidence support development in an environment removed from the surface but still influenced by an overlying regime of evaporite deposition, possibly early burial. The parallelism of vein orientation to regional structural trends suggests that halite veins developed under the influence of the regional state of stress.

Calcite and anhydrite veins present in the Wichita and Wolfcamp strata are sporadically distributed. Unfilled fractures are also observed in these strata. The origin of these features is not well-understood.

23  
SUPERSEDED

DRAFT

## ACKNOWLEDGMENTS

This research was funded by the U. S. Department of Energy, Contract No. DE-AC97-83WM46651. Many helpful comments were made by reviewers R. T. Budnik, G. E. Fogg, T. C. Gustavson, J. G. Price, J. R. DuBar, and \_\_\_\_\_. S. D. Hovorka and S. C. Ruppel supervised the many research assistants who described core utilized in this study. Cartography was by \_\_\_\_\_ under the supervision of R. L. Dillon. The following persons helped prepare this report for publication: \_\_\_\_\_.

Supplemental

**DRAFT**

## REFERENCES

- Babcock, E. A., 1978, Measurement of subsurface fractures from dipmeter logs: American Association of Petroleum Geologists Bulletin, v. 62, no. 7, p. 1111-1126.
- Bachman, G. O. 1980, Regional geology and Cenozoic history of Pecos region, Southeastern New Mexico: United States Geological Survey, Open-File Report 80-1099, 116 p.
- Bates, R. L., and Jackson, J. A., 1980, Glossary of geology, second edition: American Geological Institute, Falls Church, Virginia, p. 334.
- Beck, J., Schultz, A., and Fitzgerald, D., 1977, Reservoir evaluation of fractured Cretaceous carbonates in south Texas: SPWLA Eighteenth Annual Logging Symposium, Transactions, June 5-8, Houston, Texas, 25 p.
- Berkstresser, C. F., Jr., and Maurant, W. A., 1966, Ground water resources and geology of Quay County, New Mexico: New Mexico Bureau of Mines and Mineral Resources, Groundwater Report 9, 115 p.
- Brown, R. O., 1978, Application of fracture identification logs in the Cretaceous of North Louisiana and Mississippi: Gulf Coast Association of Geological Societies, Transactions, v. 28, p. 75-91.
- Budnik, R T., 1984, Structural geology and tectonic history of the Palo Duro Basin, Texas Panhandle: The University of Texas at Austin, Bureau of Economic Geology, Open-File Report.
- Chapman, C. A., 1958, Control of jointing by topography: Journal of Geology, v. 66, no. 5, p. 552-558.
- Cook, A. C., and Johnson, K. R., 1970, Early joint formation in sediment: Geology Magazine, v. 107, no. 4, p. 361-368.
- Dellwig, L. F., 1968, Significant features of deposition in the Hutchinson Salt, Kansas, and their interpretation, in Mattox, R. B., ed., Saline deposits: Geological Society of America, Special Paper 88, p. 421-426.

**SUPERSEDED**  
23

**DRAFT**

- Dix, O. R. and Jackson, M. P. A., 1981, Statistical analysis of lineaments and their relation to fracturing, faulting, and halokinesis in the East Texas Basin: The University of Texas at Austin, Bureau of Economic Geology Report of Investigations No. 110, 30 p.
- Dobrovolny, E., Summerson, C. H., and Bates, R. L., 1946, Geology of northwestern Quay County, New Mexico: U.S. Geological Survey, Oil and Gas Investigations, Preliminary Map No. 62.
- Dutton, S. P., 1980, Depositional systems and hydrocarbon resource potential of the Pennsylvanian system, Palo Duro and Dalhart Basins, Texas Panhandle: The University of Texas at Austin, Bureau of Economic Geology Geological Circular 80-8, 49 p.
- Eifler, G. K., Jr., 1969, Amarillo sheet: The University of Texas at Austin, Bureau of Economic Geology Geologic Atlas of Texas, scale 1:250,000, V. E. Barnes, Project Coordinator.
- Goldstein, A. G., 1982, Brittle deformation associated with salt dissolution, Palo Duro Basin, in Gustavson, T. C., and others, Geology and geohydrology of the Palo Duro Basin, Texas Panhandle, a report on the progress of nuclear waste isolation feasibility studies (1981): The University of Texas at Austin, Bureau of Economic Geology Geological Circular 81-3, p. 5-9.
- Goldstein, A. G., and Collins, E. W., 1984, Deformation of Permian strata overlying a zone of salt dissolution and collapse in the Texas Panhandle: *Geology*, v. 12, no. 5, p. 314-317.
- Gustavson, T. C., and Budnik, R. T., 1985, Structural influences on geomorphic processes and physiographic features, Texas Panhandle: technical issues in siting a nuclear-waste repository: *Geology*, v. 13, no. 3, p. 173-176.
- Gustavson, T. C., Simpkins, W. W., Alhades, A., and Hoadley, A., 1982 Evaporite dissolution and development of karst features on the Rolling Plains of the Texas Panhandle: *Earth Surface Processes and Landforms*, v. 7, p. 545-563.
- Gustavson, T. C., Finley, R. J., and McGillis, K. A., 1980, Regional dissolution of Permian Salt in the Anadarko, Dalhart, and Palo Duro Basins of the Texas Panhandle: The University of Texas at Austin, Bureau of Economic Geology Report of Investigations No. 106, 40 p.

- Handford, C. R., 1981, Bromide geochemistry of Permian Halite in the Randall County Core, in Gustavson and others, Geology and geohydrology of the Palo Duro Basin, Texas Panhandle, a report on the progress of nuclear waste isolation feasibility studies (1980): The University of Texas at Austin, Bureau of Economic Geology Geological Circular 81-3, p. 75-80.
- Handford, C. R., 1982, Sedimentology and evaporite genesis in a Holocene continental-sabkha playa basin--Bristol Dry Lake, California: Sedimentology, v. 29, p. 239-253.
- Handford, C. R., and Dutton, S. P., 1980, Pennsylvanian-Early Permian depositional systems and shelf-margin evolution, Palo Duro Basin, Texas: American Association of Petroleum Geologists Bulletin, v. 64, no. 1, p. 88-106.
- Harris, J. F., Taylor, G. L., and Walper, J. L., 1960, Relation of deformational fractures in sedimentary rocks to regional and local structure: American Association of Petroleum Geologists Bulletin, v. 44, no. 12, p. 1853-1873.
- Hobbs, D. W., 1967, The formation of tension joints in sedimentary rocks: an explanation: Geology Magazine, v. 104, no., 6, p. 550-556.
- Hodgson, R. A., 1961, Regional study of jointing in Comb Ridge-Navajo Mountain area, Arizona and Utah: American Association of Petroleum Geologists Bulletin, v. 45, no. 1, p. 1-38.
- Holdaway, K. A., 1978, Deposition of evaporites and red beds of the Nippewalla Group, Permian, western Kansas: The University of Kansas, Lawrence, Kansas, Kansas Geological Survey, Bulletin 215, 43 p.
- Holser, W. T., Wardlaw, N. C., and Watson, D. W., 1972, Bromide in salt rocks: extraordinarily low content in the Lower Elk Point salt, Canada, in Geology of saline deposits, Hanover Symposium Proceedings, 1968: Earth Sciences, v. 7, p. 69-75.
- Hovorka, S. D., 1983, Sedimentary structures and diagenetic modifications in halite and anhydrite, Palo Duro Basin, in Gustavson, T. C. and others, Geology and geohydrology of the Palo Duro Basin, Texas Panhandle: The University of Texas at Austin, Bureau of Economic Geology Geological Circular 83-4, p. 49-57.

25  
SUPERSEDED

DRAFT

- Hunt, C. B., Robinson, T. W., Bowles, W. A., and Washburn, A. L., 1966, Hydrologic basin, Death Valley, California: U.S. Geological Survey Professional Paper 494-B, 138 p.
- Kulander, B. R., Barton, C. C., and Dean, S. L., 1979, The application of fractography to core and outcrop fracture investigations: prepared for U. S. Department of Energy, Morgantown Energy Technology Center, METC/SP-79/3, 174 p.
- Lovelace, A. D., 1972a, Grady Quadrangle, in Geology and aggregate resources of District II: New Mexico State Highway Department, scale 1:190,080, p. 60.
- Lovelace, A. D., 1972b, Ragland Quadrangle, in Geology and aggregate resources of District II: New Mexico State Highway Department, scale 1:190,080, p. 59.
- McGowen, J. H., Granata, G. E., and Seni, S. J., 1979, Depositional framework of the Lower Dockum Group (Triassic), Texas Panhandle: The University of Texas at Austin, Bureau of Economic Geology Report of Investigations No. 97, 60 p.
- Nelson, R. A., 1979, Natural fracture systems: description and classification: American Association of Petroleum Geologists, v. 63, no. 12, p. 2214-2221.
- Parker, J. M., 1942, Regional systematic jointing in slightly deformed sedimentary rocks: Geological Society of America Bulletin, v. 53, no. 3, p. 381-408.
- Powers, S., 1922, Reflected buried hills and their importance in petroleum geology: Economic Geology, v. 17, no. 4, p. 233-259.
- Presley, M. W., 1981, Middle and Upper Permian salt-bearing strata of the Texas Panhandle: lithologic and facies cross sections: The University of Texas at Austin, Bureau of Economic Geology Cross Sections, 10 p.
- Price, N. J., 1966, Fault and joint development in brittle and semi-brittle rock: New York, Pergamon Press, 176 p.
- Price, N. J., 1974, The development of stress systems and fracture patterns in undeformed sediments, in Advances in Rock Mechanics: Washington, D.C., National Academy of Sciences, v. 1, Part 1, p. 487-496.

**SUPPLEMENT**

**DRAFT**

- Ramsay, J. G., and Huber, M. I., 1983, The techniques of modern structural geology, volume 1: strain analysis: London, Academic Press, 307 p.
- Rogatz, H., 1939, Geology of Texas Panhandle oil and gas field: American Association of Petroleum Geologists Bulletin, v. 23, no. 7, p. 983-1053.
- Sangree, J. B., 1969, What you should know to analyze core fractures: World Oil, v. 168, no. 5, p. 69-72.
- Schlumberger, 1981, Dipmeter interpretations, volume 1: New York, Schlumberger Limited, 61 p.
- Seni, S. J., 1980, Sand-body geometry and depositional systems, Ogallala Formation, Texas: The University of Texas at Austin, Bureau of Economic Geology Report of Investigations No. 105, 36 p.
- Simpkins, W. W., Gustavson, T. C., Alhades, A. B., and Hoadley, A. D., 1981, Impact of evaporite dissolution and collapse on highways and other cultural features in the Texas Panhandle and Eastern New Mexico: The University of Texas at Austin, Bureau of Economic Geology Geological Circular 81-4, 23 p.
- Spencer, A. M., and Spencer, M. O., 1972, The late Precambrian/Lower Cambrian Bonahaven Dolomite of Islay and its stromatolites: Scottish Journal of Geology, v. 8, p. 269-282.
- Stearns, D. W., 1972, Structural interpretation of the fractures associated with the Bonita Fault, in Guidebook of East-Central New Mexico: New Mexico Geological Society, Twenty-third field conference, p. 161-164.
- Stearns, D. W., and Freidman, M., 1972, Reservoirs in fractured rock, in Stratigraphic oil and gas fields--classification, exploration methods, and case histories: American Association of Petroleum Geologists Memoir 16, p. 82-106.
- Totten, R. B., Jr., 1956, General geology and historical development, Texas and Oklahoma Panhandles: American Association of Petroleum Geologists Bulletin, v. 40, no. 8, p. 1945-1967.

**SUPERSEDED**  
27

**DRAFT**

- Tucker, R. M., 1981, Giant polygons in the Triassic salt of Cheshire, England: A thermal contraction model for their origin: *Journal of Sedimentary Petrology*, v. 51, p. 779-786.
- Van Houten, F. B., 1964, Cyclic lacustrine sedimentation, Upper Triassic Lockatong Formation, Central New Jersey and adjacent Pennsylvania, in Merriam, D. F., ed., Symposium on cyclic sedimentation: *Bulletin Kansas Geological Survey*, v. II, no. 169, p. 497-531.
- Wardlaw, N. C., and Watson, D. W., 1966, Middle Devonian salt formations and their bromide content, Elk Point Area, Alberta: *Canadian Journal of Earth Sciences*, v. 3, p. 263-275.
- Winchester, D. E., 1933, The oil and gas resources of New Mexico: *New Mexico School of Mines, State Bureau of Mines and Mineral Resources, Bulletin No. 9*, p. 133-134.
- Wise, D. U., and McCrory, T. A., 1982, A new method of fracture analysis: azimuth versus traverse distance plots: *Geological Society of American Bulletin*, v. 93, no. 9, p. 889-897.

28  
SUPERSEDED

**DRAFT**

## Figure Captions

Figure 1. Structural setting of the Palo Duro Basin area showing the location of (1) stations for the regional joint and Fracture Identification Log (FIL) fracture measurements and (2) areas for detailed field studies.

Figure 2. Stratigraphic column and general lithology of the Palo Duro and Dalhart Basins. After Hanford and Dutton (1980). Alibates, upper Clear Fork, Tubb, lower Clear Fork, and Red Cave have been informally designated as formations.

Figure 3. Fracture maps of the Texas Panhandle and eastern New Mexico region showing (a) mean fracture strikes for Permian strata, (b) mean fracture strikes that are significant at 95% confidence for Permian strata, (c) mean fracture strikes for Triassic strata and (d) mean fracture strikes that are significant at 95% confidence. Stations for fracture measurements and structural setting are shown in figure 1.  $n$  = the number of measurements in each quadrant.

Figure 4. (a) Strikes of faults and joints at the western margin of the Palo Duro Basin in eastern New Mexico. Rose diagram data are plotted as percentages of total number of measurements ( $n$ ) for  $10^\circ$  intervals. (b) Structure contour map on base of the Permian San Andres Formation in Quay, Curry, and Roosevelt Counties, eastern New Mexico.

Figure 5. (a) Location of study area at flank of John Ray Dome. (b) Location of traverses in Permian strata (P), Triassic strata (Tr), and Tertiary strata (T).

Figure 6. Azimuth-versus-traverse-distance plots are for joints in (a) Tertiary, (b) Triassic, (c) Permian strata.  $N$  = number of measurements,  $S$  = number of stations, STA = selected station number, and  $D$  = average distance between the stations. Contours are in concentration of data within  $10^\circ$  intervals across every  $2^\circ$  of azimuth (Wise and McCrory, 1982). Corresponding rose diagram plots are of joints in (d) Tertiary, (e) Triassic, and (f) Permian strata. Data are plotted as percentages of total number of measurements ( $N$ ) for  $10^\circ$  intervals.

Figure 7. Lower hemisphere equal area net plots for poles to (a) shear fractures in Triassic sandstone and (b) normal faults in Tertiary sandstone and conglomerate. Contours are in percent per one percent area.

**SUPERSEDED**

**DRAFT**

Figure 8. Location of traverses in Triassic (Tr), Jurassic (Jr), and Cretaceous (K) strata at the San Jon Hill locality, Quay County, New Mexico. AVTD plots for the traverses are shown in figure 9.

Figure 9. Azimuth-versus-traverse-distance plots are for joints in (a) Triassic, (b) Jurassic, (c) Cretaceous strata. N = number of measurements, S = number of stations, STA = selected station number, and D = average distance between the stations. Contours are in concentration of data within  $10^\circ$  intervals across every  $2^\circ$  of azimuth (Wise and McCrory, 1982). Corresponding rose diagram plots are of joints in (d) Triassic, (e) Jurassic, and (f) Cretaceous strata. Data are plotted as percentages of total number of measurements (N) for  $10^\circ$  intervals.

Figure 10. Fracture identification log (FIL) in Permian Wolfcamp strata for Stone & Webster-J. Friemel #1 borehole.

Figure 11. Location of boreholes used for fracture studies in the Palo Duro Basin area.

Figure 12. Frequency distributions of FIL fracture orientations for Deaf Smith County in (a) Pennsylvanian strata, (b) Permian strata, (c) cored intervals of Permian strata, (d) Triassic strata, and (e) Tertiary strata. Data for figure 12a are from the Stone & Webster-J. Friemel #1 borehole, whereas for figures 12b, 12c, 12d, and 12e the data are from the Stone & Webster-J. Friemel #1, G. Friemel #1, and Detten #1 boreholes. Data have been smoothed by 10! running average every  $2^\circ$  of azimuth (Wise and McCrory, 1982, p. 893).

Figure 13. Histograms showing fracture orientations (a) in cored intervals of Permian strata in Deaf Smith County, (b) of vein-filled fractures, and (c) of fractures with no vein fillings. Data have been smoothed by  $10^\circ$  running average every  $2^\circ$  of azimuth (Wise and McCrory, 1982, p. 893).

Figure 14. Frequency distributions of FIL fracture orientations for Swisher County in (a) Pennsylvanian strata, (b) Permian strata, (c) cored intervals of Permian strata, and (d) Triassic strata. Data for figure 14a are from the Stone & Webster-Zeeck #1 borehole, whereas for figures 14b and 14c the data are from the Stone & Webster-Zeeck #1 and Harman #1 boreholes.

**SUPERSEDED**  
2

**DRAFT**

Figure 14d data are joint measurements from outcrop. All data have been smoothed by 10! running average every 2° of azimuth (Wise and McCrory, 1982, p. 893).

Figure 15. Cross-section view of a joint zone extending through Permian and Triassic rocks at Caprock Canyons State Park in Briscoe County. Overlying Tertiary Ogallala sediments are also fractured, although it is uncertain if the Ogallala fractures are actually systematic joints that are part of the joint zone.

Figure 16. Graph showing weighted joint density versus log of bed thickness for data from Caprock Canyons State Park, Palo Duro Canyon State Park, and joint zones at both parks. Joint densities were double weighted to smooth the raw data (Jackson, personal instruction, 1983).

The first weighting is based on binomial coefficients on the 3rd ( $a + b^2$ ) and 5th ( $a + b^4$ ) rows of Pascal's triangle. The second weighting is based on the number of readings ( $N_i$ ) in the particular interval. The expression used for smoothing the data is as follows:

$$\text{double weighted mean joint density} = \bar{X}_m + \frac{\sum_{i=1}^N (\bar{X}_i - \bar{X}_m) \times (y_i/y_m) \times (n_i/n_m)}{N}$$

- $\bar{X}_m$  = arithmetic mean of middle interval
- $\bar{X}_i$  = arithmetic mean of neighboring intervals
- $y_m$  = binomial coefficient of middle interval
- $y_i$  = binomial coefficient of neighboring intervals
- $n_m$  = number of readings in middle interval
- $n_i$  = number of readings in neighboring intervals
- $N$  = number of intervals combined (3 or 5)

Five intervals were used for smoothing the data except at the ends of the curve where three intervals were used. The coefficients for five intervals are 14641 (5th row, Pascal's triangle). Coefficients for three intervals are 121 (3rd row, Pascal's triangle).

3  
SUPERSEDED

**DRAFT**

Figure 17. Location of traverses in Permian strata at Palo Duro Canyon State Park. AVTD plots for the traverses are shown in figure 19.

Figure 18. Azimuth-versus-traverse-distance plots are for joints in Permian strata at Palo Duro Canyon State Park, Randall County, Texas. N = number of measurements, S = number of stations, STA = station number, and D = average distance between the stations. Contours are in concentration of data within 10° intervals across every 2° of azimuth (Wise and McCrory, 1982). Corresponding rose diagram plots are of joints measured at each traverse. Data are plotted as percentages of total number of measurements (N) for 10° intervals.

Figure 19. Photograph showing a cave that has formed where the joint density is higher than the surrounding areas. The cave is located at Palo Duro Canyon State Park, Randall County. The width of the cave is 3.5 m.

Figure 20. Photograph showing dissolution along fractures in Permian gypsum bed at Palo Duro Canyon State Park, Randall County. The scale is in 1/4 m increments.

Figure 21. Graph comparing joint density and the percent of cavity lengths to the total length measured (2 m). Joint density was measured across 2 m. The horizontal lengths across cavities were measured for several 2 m lines and the mean sum of horizontal cavity lengths was divided by 2 m (total length) to determine the cavity percentages.

Figure 22. Percentage of fractured Permian core from boreholes in Oldham, Deaf Smith, and Randall Counties, Texas. Abbreviations of Permian formations are as follows: A - Alibates; S/T - Salado-Tansill; Y - Yates; SR - Seven Rivers; QG - Queen Grayburg; SA - San Andres; G - Glorieta; uCF - upper Clear Fork; T - Tubb; lCF - lower Clear Fork.

Figure 23. Composition of veins in core of Permian strata from salt dissolution zone.

Figure 24. Composition of veins in core of Permian salt-bearing strata.

Figure 25. Composition of veins in core of the Red Cave Formation and Wichita and Wolfcamp Groups. These units are stratigraphically below the Permian salt-bearing units.

**SUPERSEDED**

**DRAFT**

Figure 26. Gypsum-filled fractures. Fibers are oriented perpendicular to fracture walls. Oblique veins cross-cut near horizontal ones. Scale in centimeters. Salado-Tansill Formation; DOE-Gruy Federal #1 Rex White.

Figure 27. Photomicrograph of medial suture zone of fibrous gypsum vein. Suture marked by finely crystalline gypsum. Width of photomicrograph is 4.1 mm. Salado-Tansill Formation; DOE-Gruy Federal #1 Rex White.

Figure 28. Anastomosing style veins in dissolution fabric host containing gypsum nodules. Salado-Tansill Formation; DOE-Gruy Federal #1 Rex White.

Figure 29. Photograph of core from DOE-Stone & Webster #1 Mansfield, depth 1374', Upper San Andres Formation. Red fibrous halite vein in insoluble residue at base of depositional cycle; fibers are oriented perpendicular to fracture walls. Width of core is 10 cm.

Figure 30. Photograph of core from DOE-Stone & Webster #1 Mansfield, depth 2930', Upper Clear Fork Formation. Red fibrous vein with sigmoidal-shaped fibers. Vein cuts through microstylolitized carbonate unit; there is no apparent distortion or disturbance of the laminae at the vein wall contact. Width of core is 10 cm.

Figure 31. Photograph of core from DOE-Stone & Webster #1 Mansfield, depth 1993', Lower San Andres Formation. Common shape of fibrous halite veins pinching out at both ends.

Figure 32. Photograph of core from DOE-Stone & Webster #1 Mansfield, depth 1373.6', Upper San Andres Formation. Photomicrograph of fractured ooids at halite vein wall contact. Plane light, width is 3.25 mm.

Figure 33. Photograph of core from DOE-Stone & Webster #1 Mansfield, depth 1375.7', Upper San Andres Formation. Photomicrograph of anhydrite nodule annealed across halite vein. Crossed nicols, width is 3.25 mm.

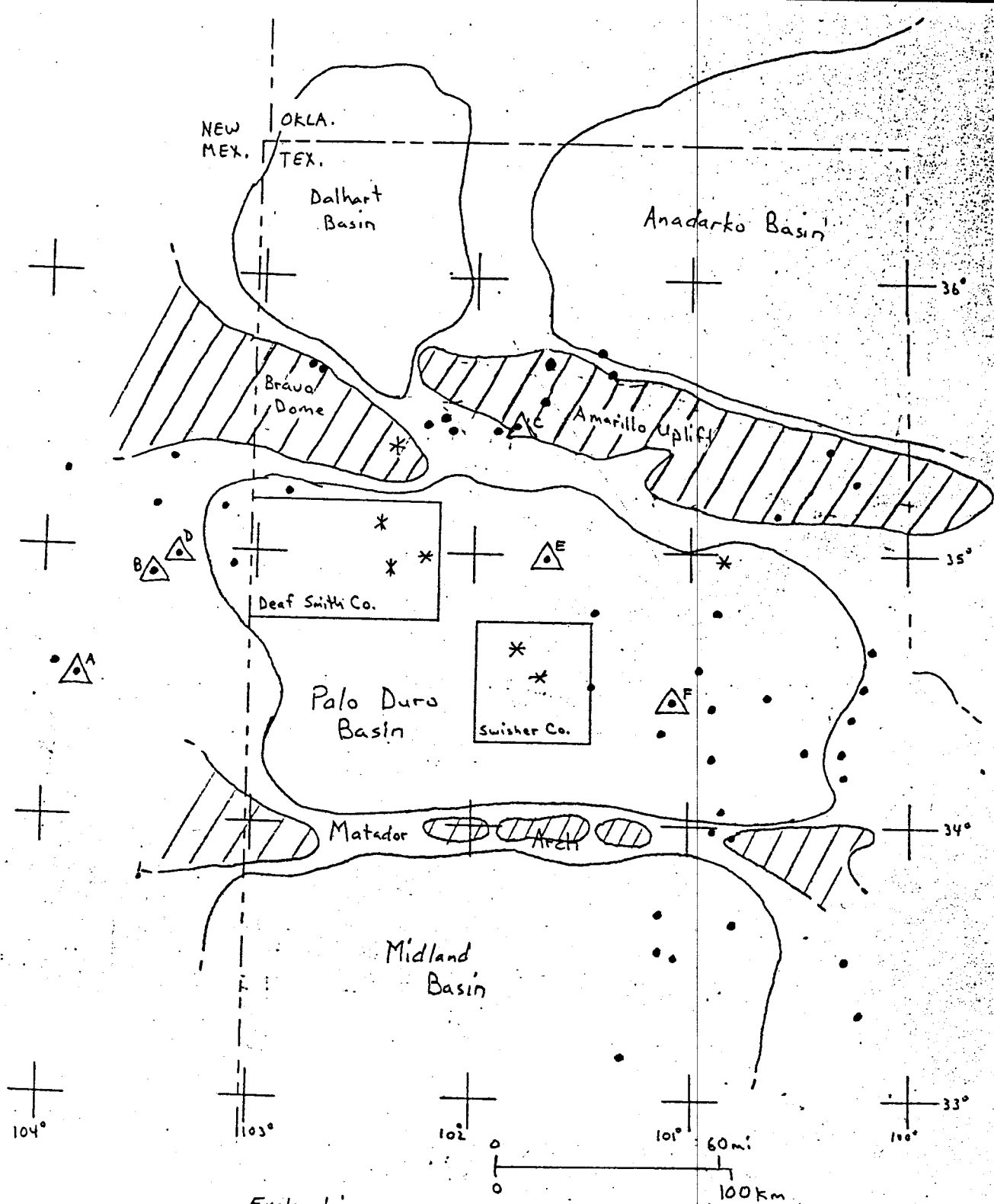
Figure 34. Bromide concentrations in bedded and recrystallized halite and vein halite. A) distribution of bromide concentrations in the upper Clear Fork, Tubb, lower Clear Fork Formations; values for undifferentiated salt are from Handford (1981) corrected for percent soluble material; B) distribution of bromide concentrations in the Lower San Andres Formation;

<sup>5</sup>  
**SUPERSEDED DRAFT**

C) distribution of bromide concentrations in the Upper San Andres Formation. All plots show similar relationship of vein bromide concentrations within the range of those for "other" salt.

**SUPERSEDED**

**DRAFT**



*Explanation*

 Area of uplift

• Station for joint measurements

\* Station for FIL fracture measurement

-  Location of:
- A Alamosa Fault
  - B Banita Fault
  - C drape fold off John Ray Dome
  - D San Jon Hill
  - E Palo Duro Canyon State Park
  - F Cap Rock Canyons State Park

Fig. 1

**SUPERSEDED**

**DRAFT**

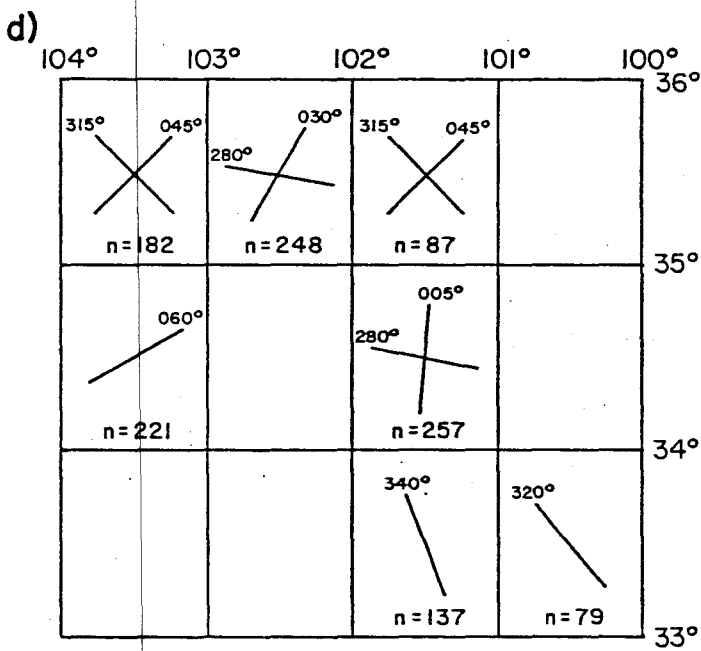
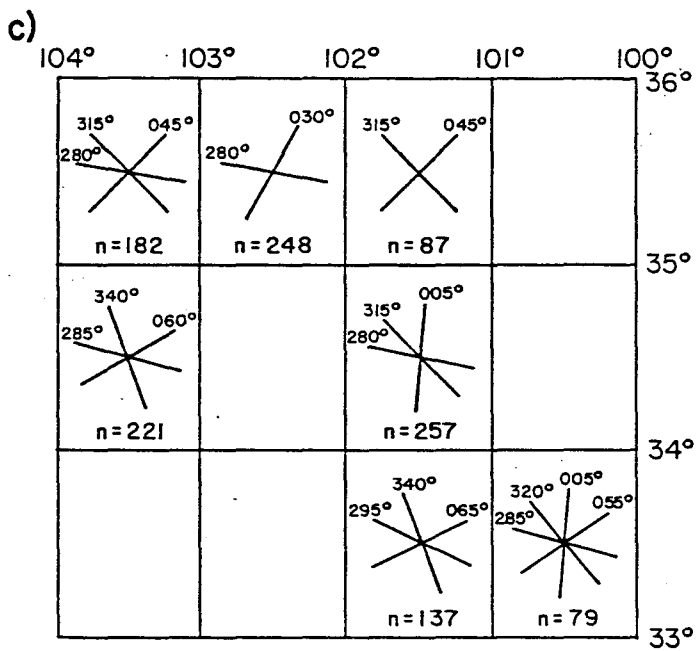
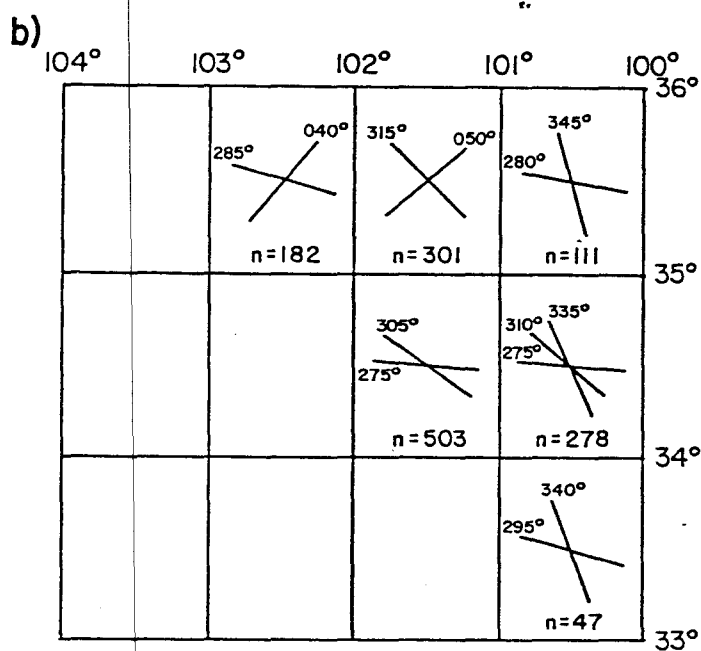
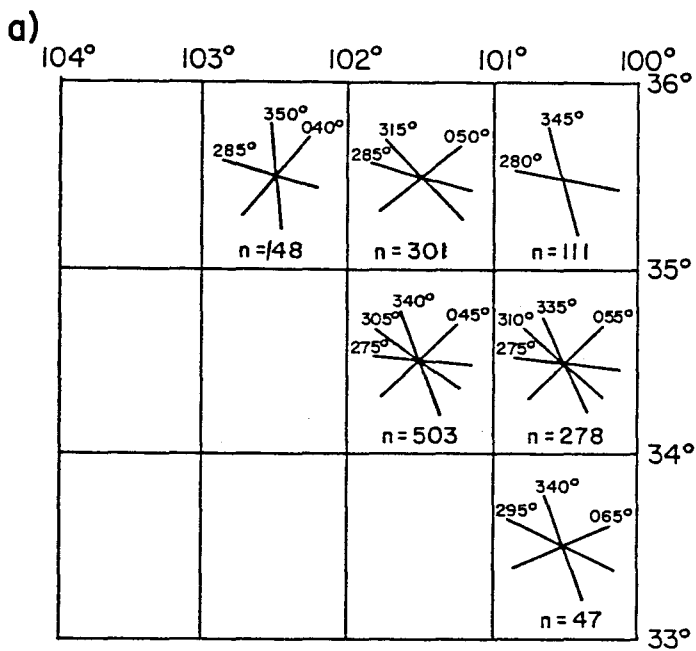
SYSTEM	SERIES	GROUP	Palo Duro Basin	Dalhart Basin	General Lithology and depositional setting	
			FORMATION	FORMATION		
QUATERNARY	HOLOCENE		alluvium, dune sand Playa	alluvium, dune sand Playa		
	PLEISTOCENE		Tahoka "cover sands" Tule / "Playa" Blanca	"cover sands" "Playa"	Lacustrine clastics and windblown deposits	
TERTIARY	NEOGENE		Ogallala	Ogallala	Fluvial and lacustrine clastics	
CRETACEOUS			undifferentiated	undifferentiated	Marine shales and limestone	
TRIASSIC		DOCKUM			Fluvial-deltaic and lacustrine clastics	
PERMIAN	OCHOA		Dewey Lake	Dewey Lake	Sabkha salt, anhydrite, red beds, and peritidal dolomite	
			Alibates	Alibates		
	GUADALUPE	ARTESIA		Salada/Tansill		Artesia Group undifferentiated
				Yates		
				Seven Rivers		
				Queen/Grayburg		
				San Andres		Blaine
	LEONARD	CLEAR FORK		Glorieta		Glorieta
				Upper Clear Fork		Clear Fork
				Tubb		undifferentiated Tubb-Wichita Red Beds
				Lower Clear Fork		
				Red Cave		
		WICHITA				
		WOLFCAMP				
PENNSYLVANIAN	VIRGIL	CISCO	?	?	Shelf and shelf-margin carbonate, basinal shale, and deltaic sandstone	
	MISSOURI	CANYON				
	DES MOINES	STRAWN				
	ATOKA	BEND				
	MORROW					
MISSISSIP- SIAN	CHESTER				Shelf carbonate and chert	
	MERAMEC					
	OSAGE					
ORDOVICIAN		ELLEN- BURGER			Shelf dolomite	
CAMBRIAN ?					Shallow marine(?) sandstone	
PRECAMBRIAN					Igneous and metamorphic	

Fig. 2

Figure 2. Stratigraphic column and general lithology of the Palo Duro and Dalhart Basins. After Handford and Dutton (1980).

SUPERSEDED

DRAFT



QA4505

Fig. 3

SUPERSEDED

DRAFT

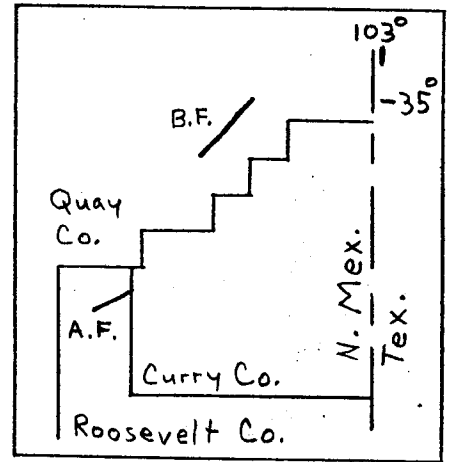
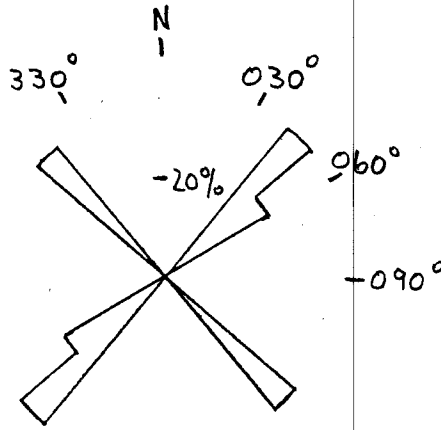
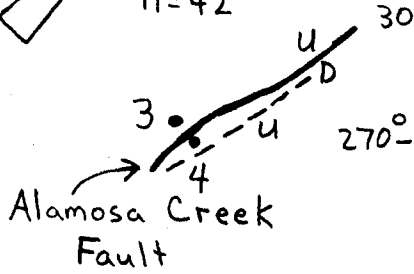
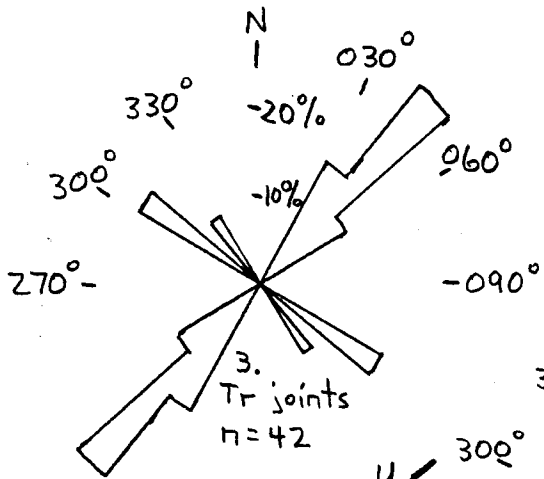
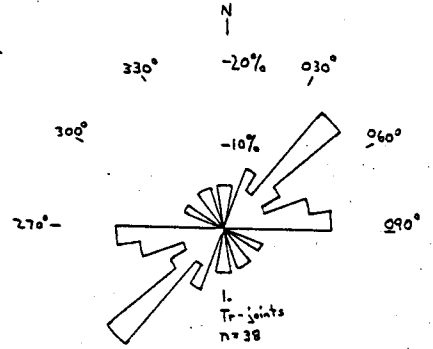
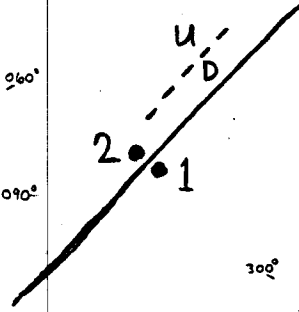
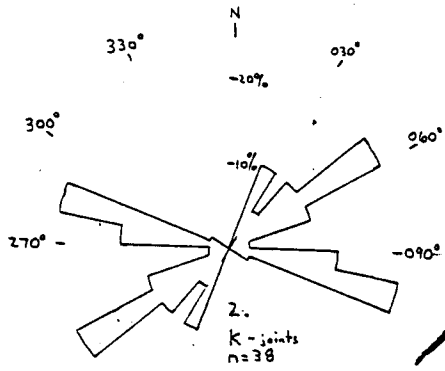
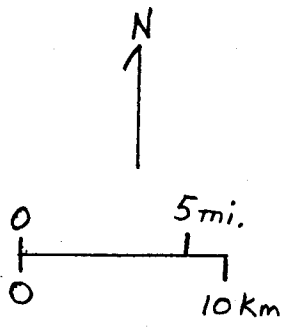


Fig. 4a

**SUPERSEDED**

**DRAFT**

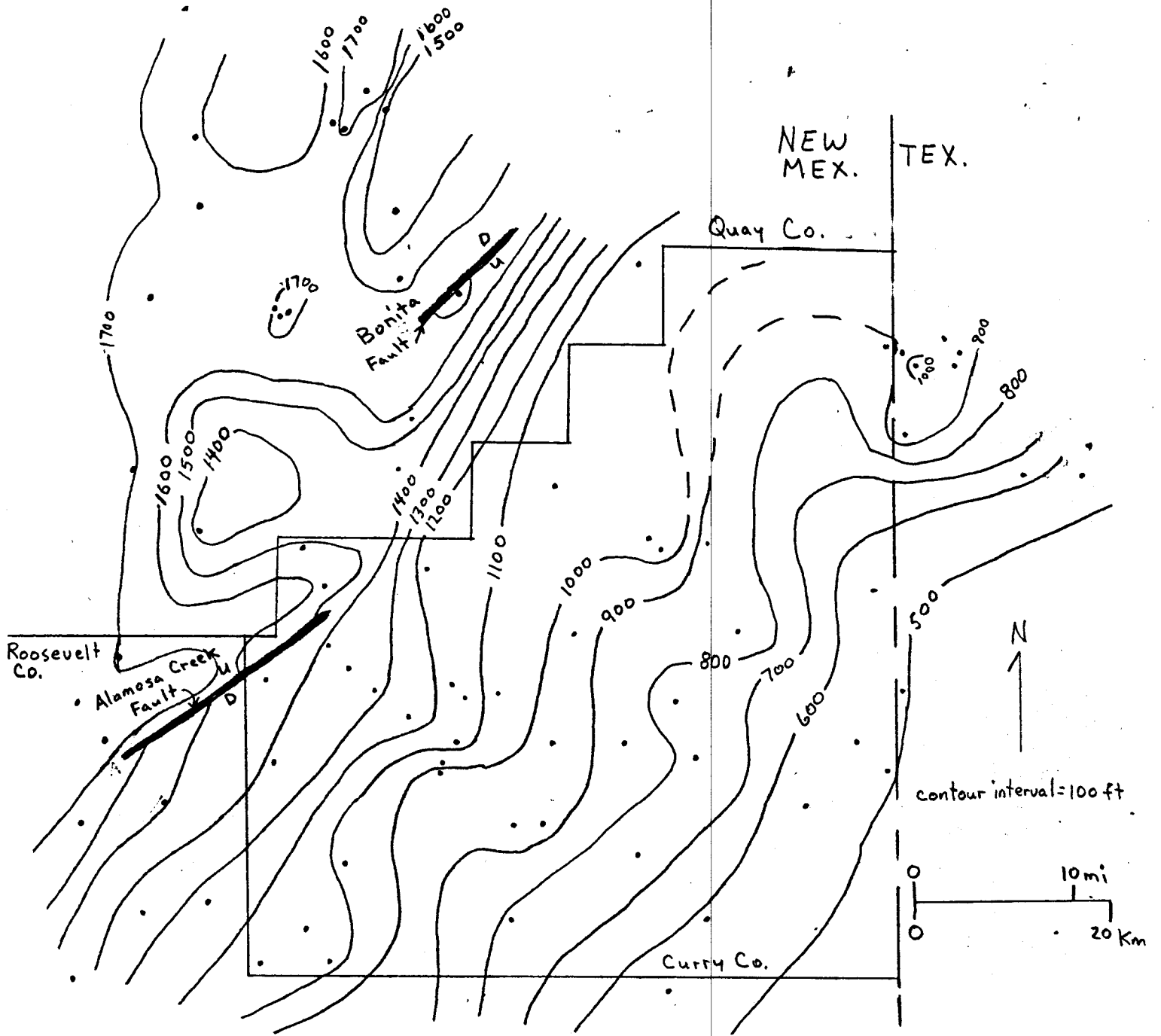


Fig. 4b

SUPERSEDED

DRAFT

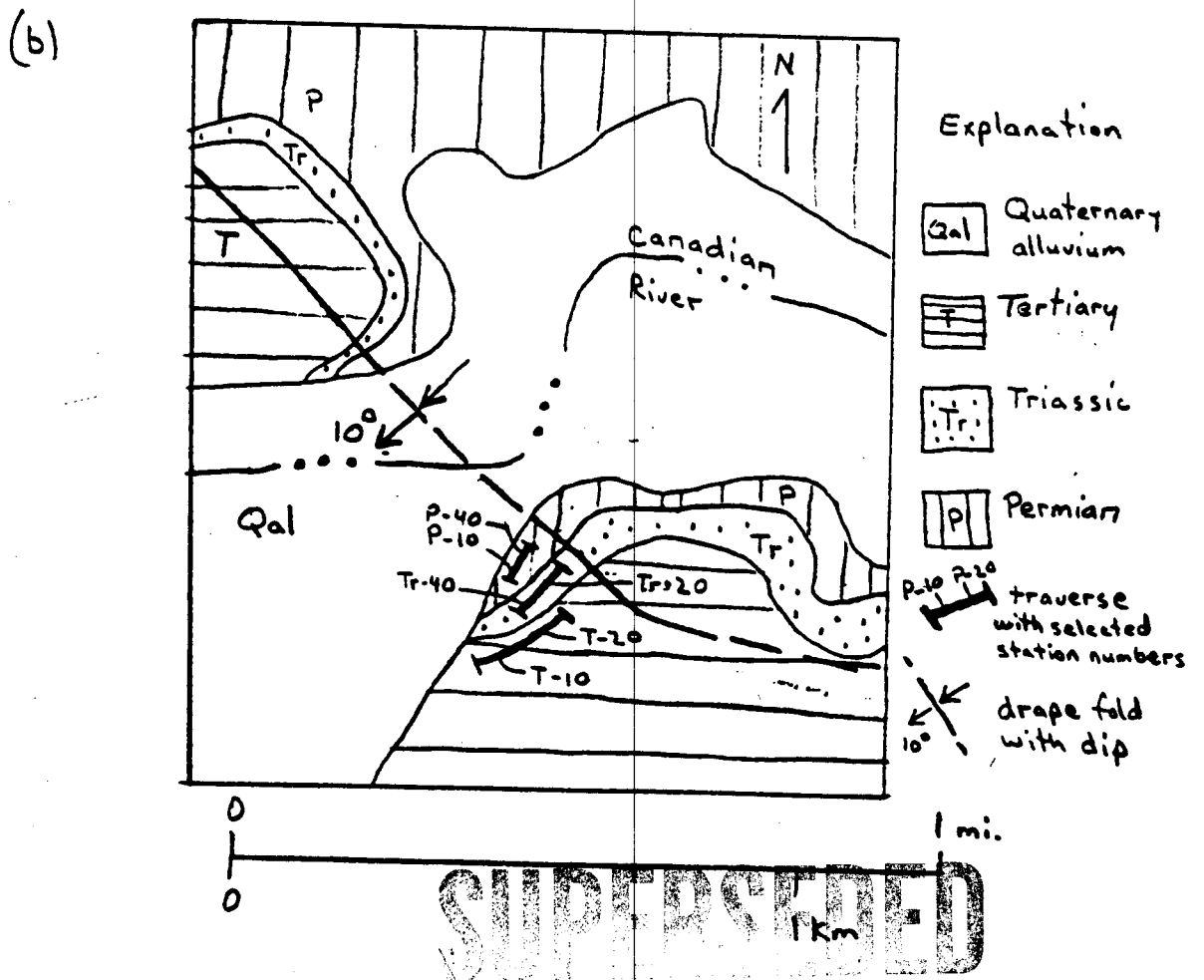
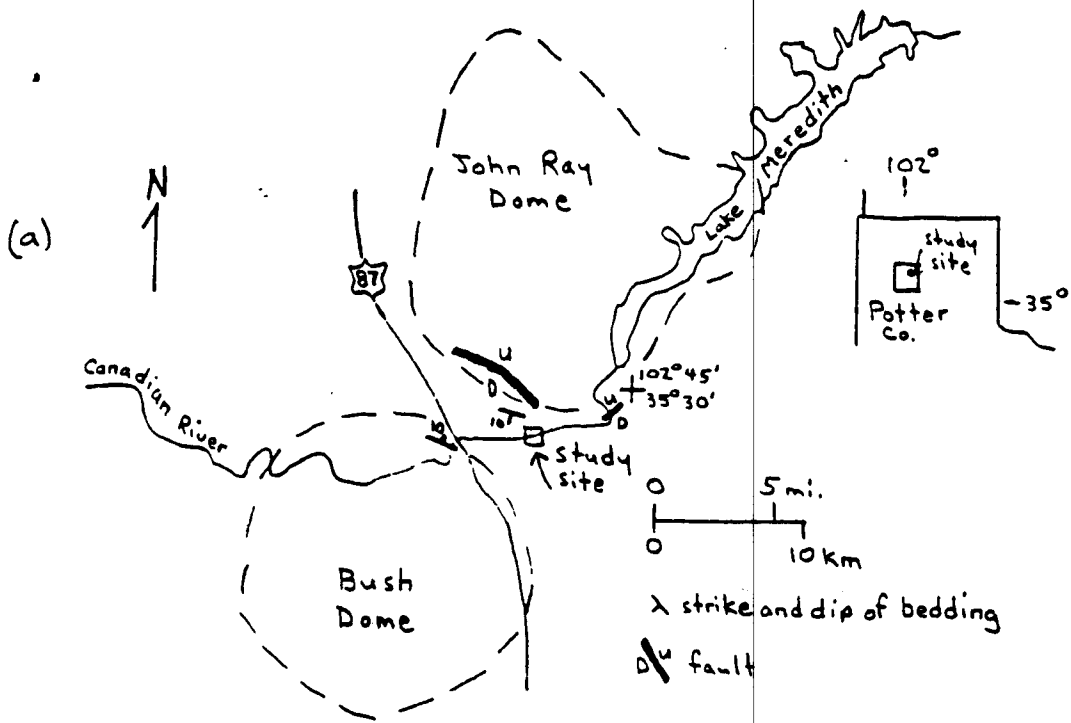
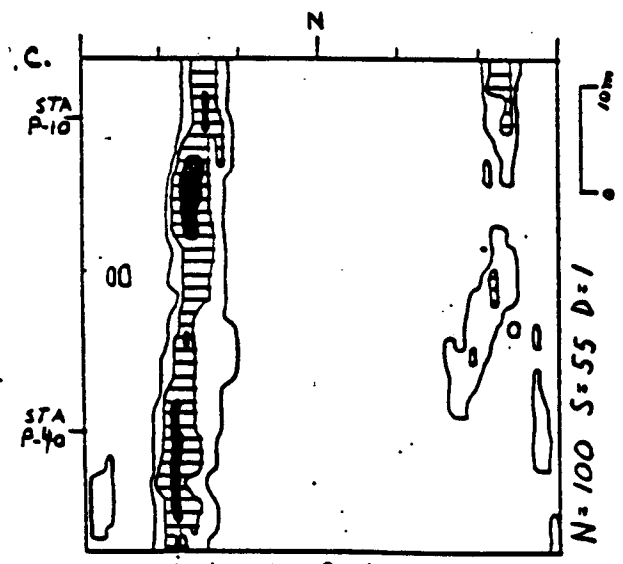
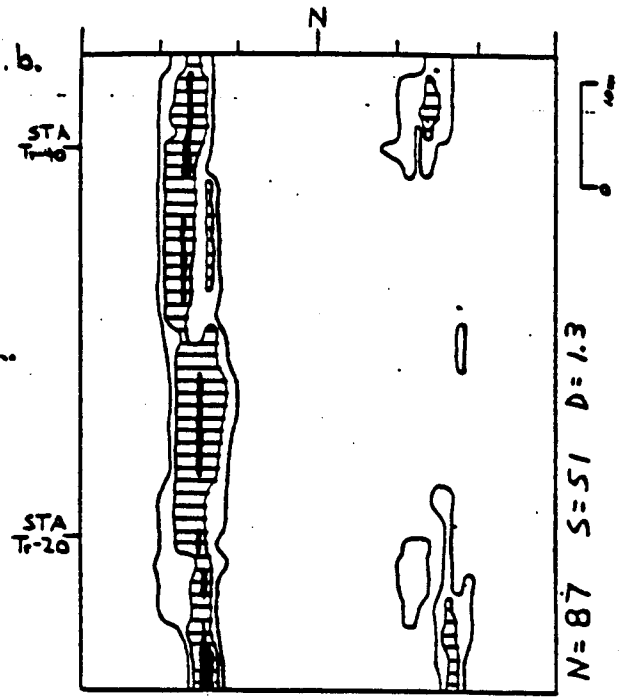
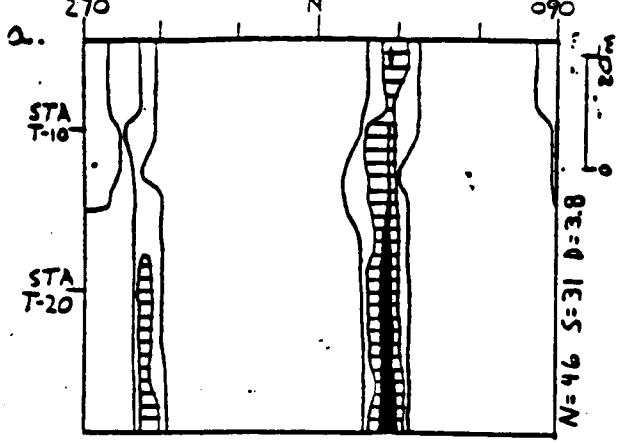


Fig. 5

**DRAFT**



Concentration factor contours:  
 3-5 □ 5-7 ▨ >7 ■

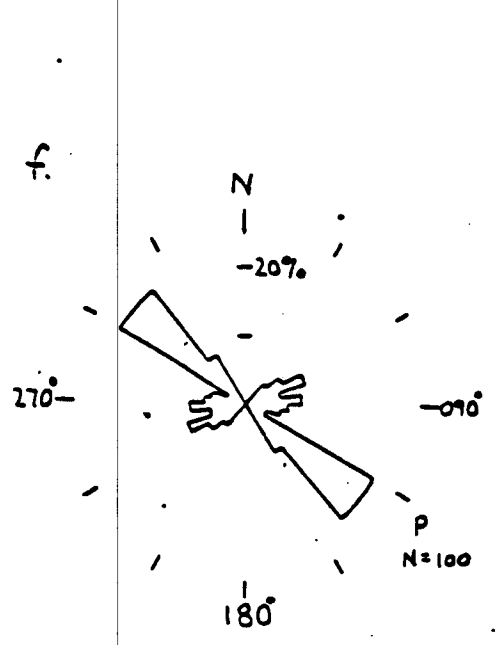
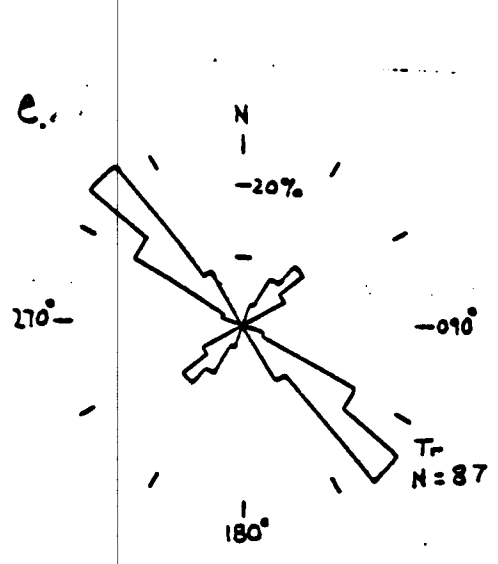
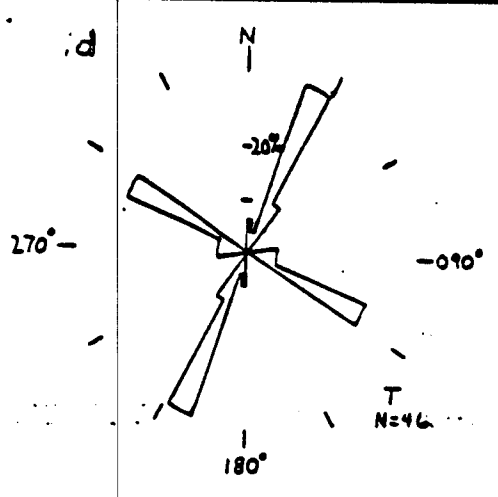
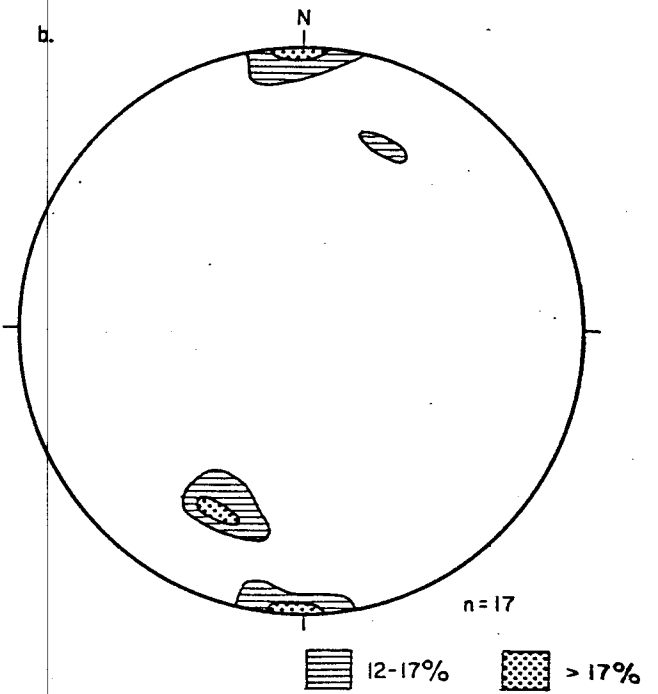
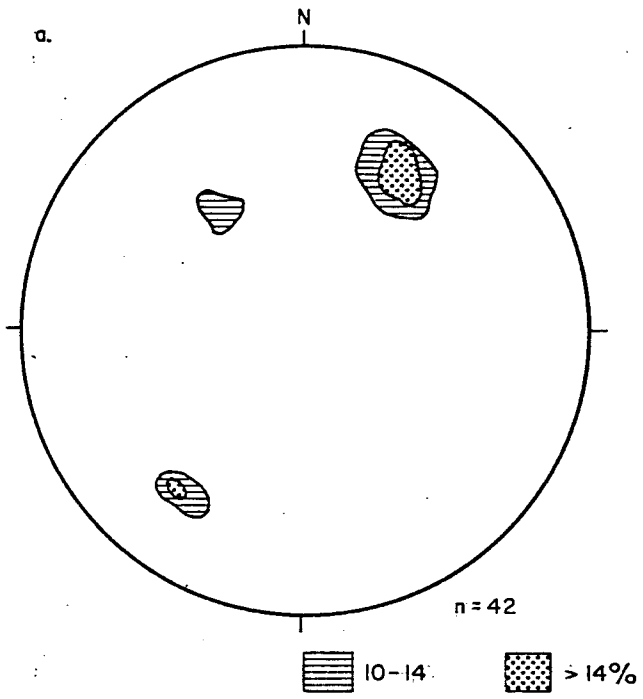


Fig. 6

**SUPERSEDED**

**DRAFT**



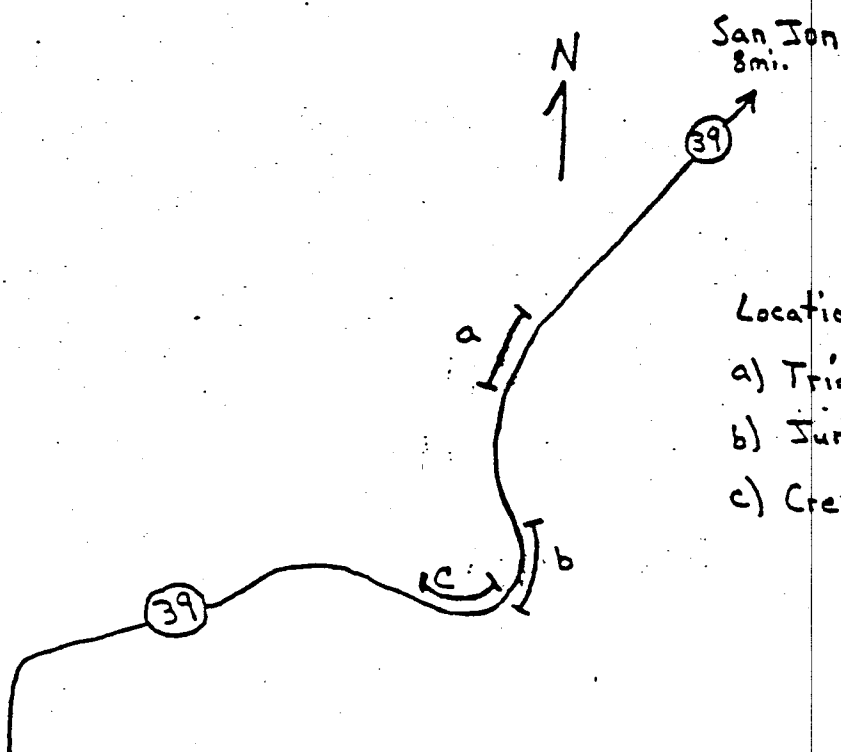
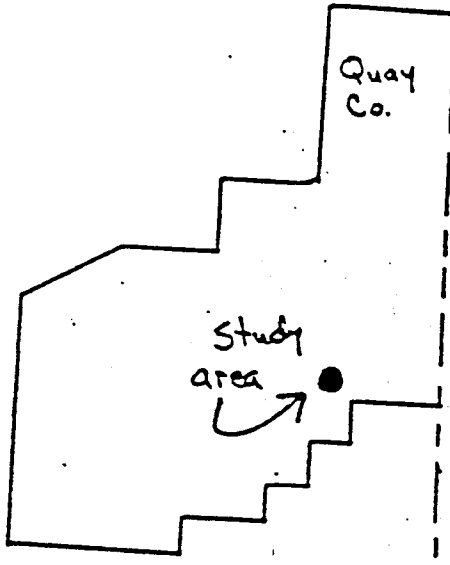
QA 4506

**SUPERSEDED**

Fig. 7

**DRAFT**

New Mex. | Tex.



Location of traverse in:

- a) Triassic rocks
- b) Jurassic rocks
- c) Cretaceous rocks

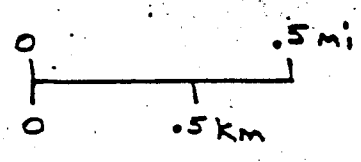
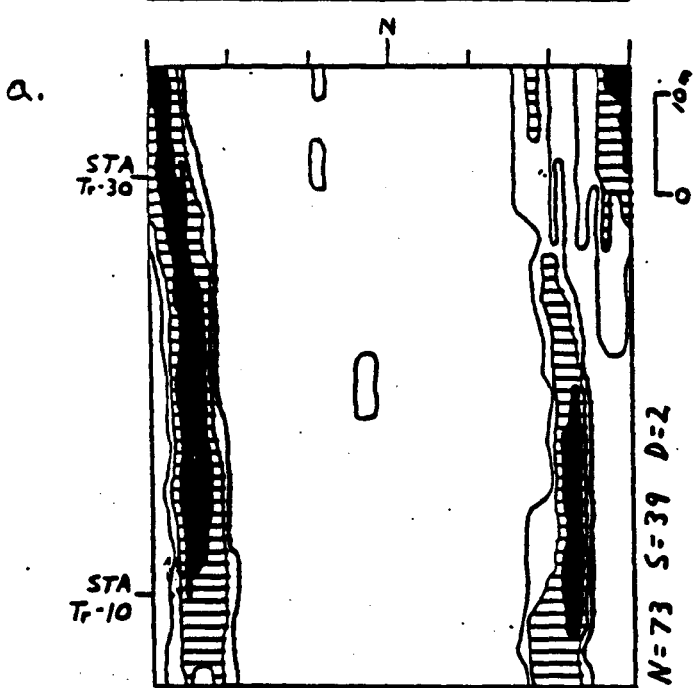
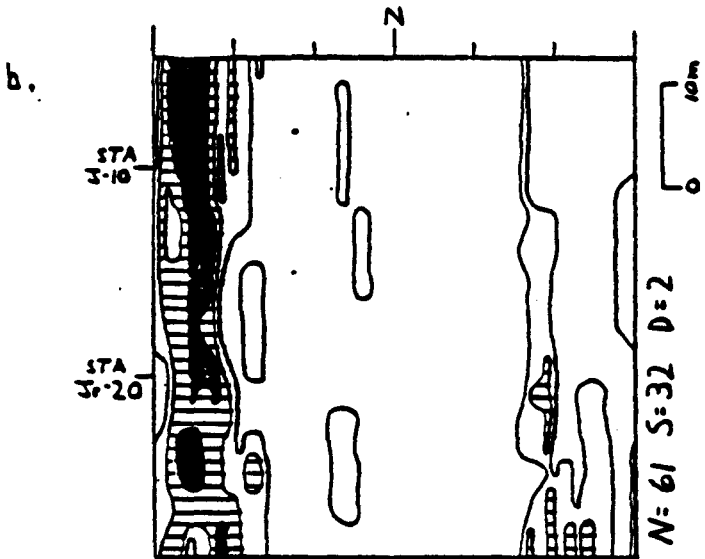
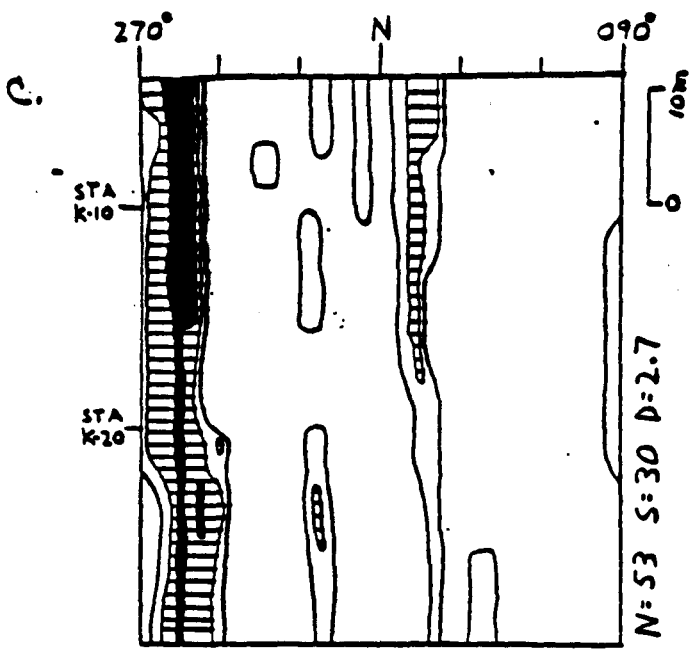


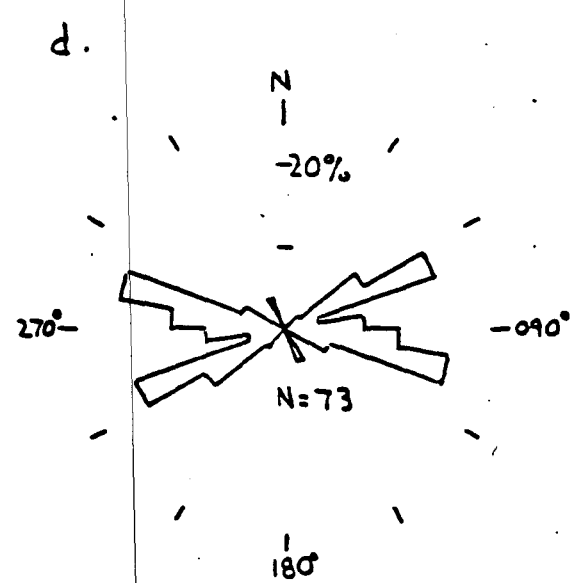
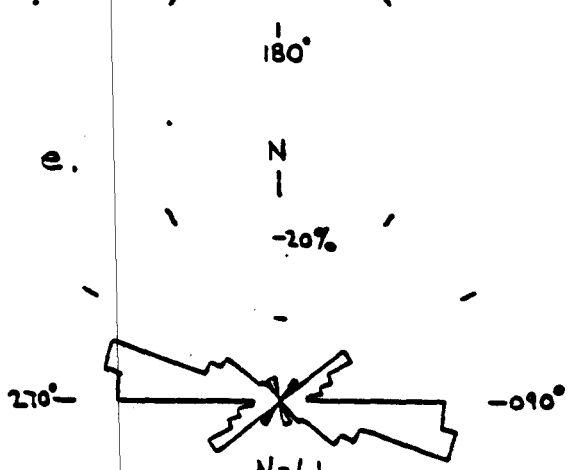
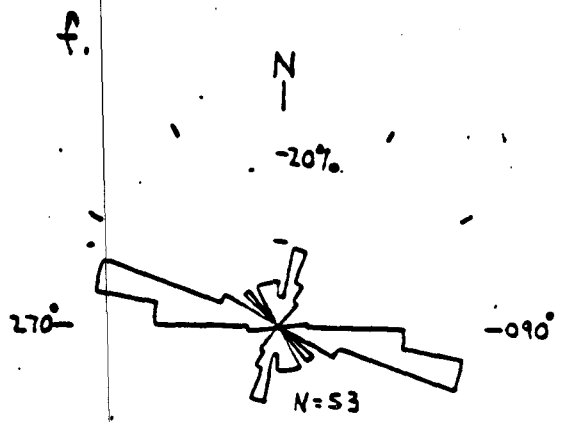
Fig. 8

**SUPERSEDED**

**DRAFT**



Concentration factor contours:  
 2-3 □ 3-5 ▨ >5 ■



**SUPERSEDED**  
 COPIED FOR QA FILES **DRAFT**

Fig. 9

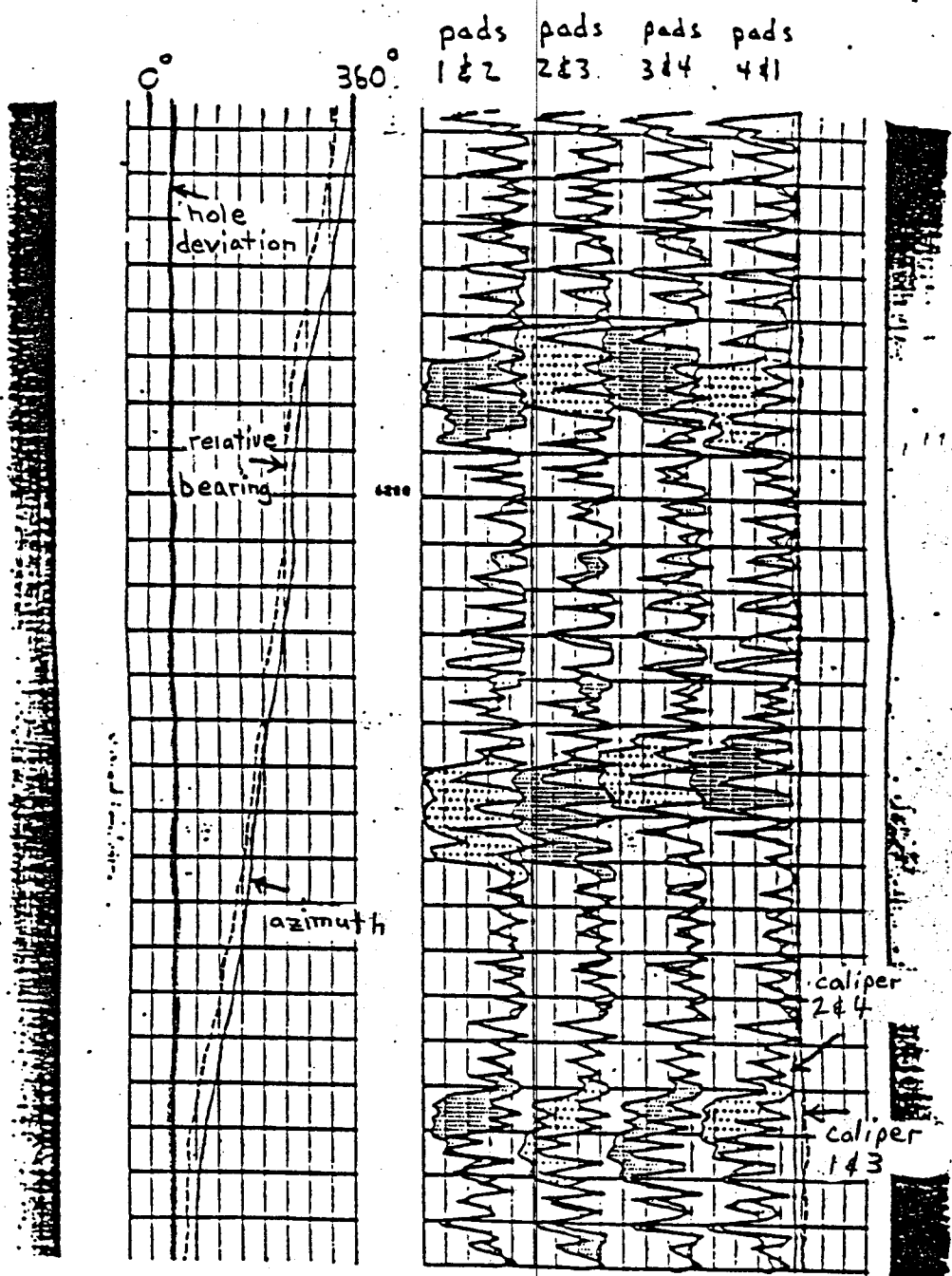
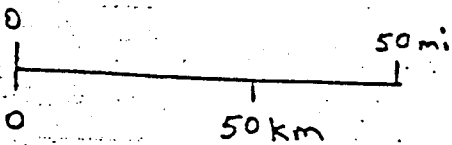
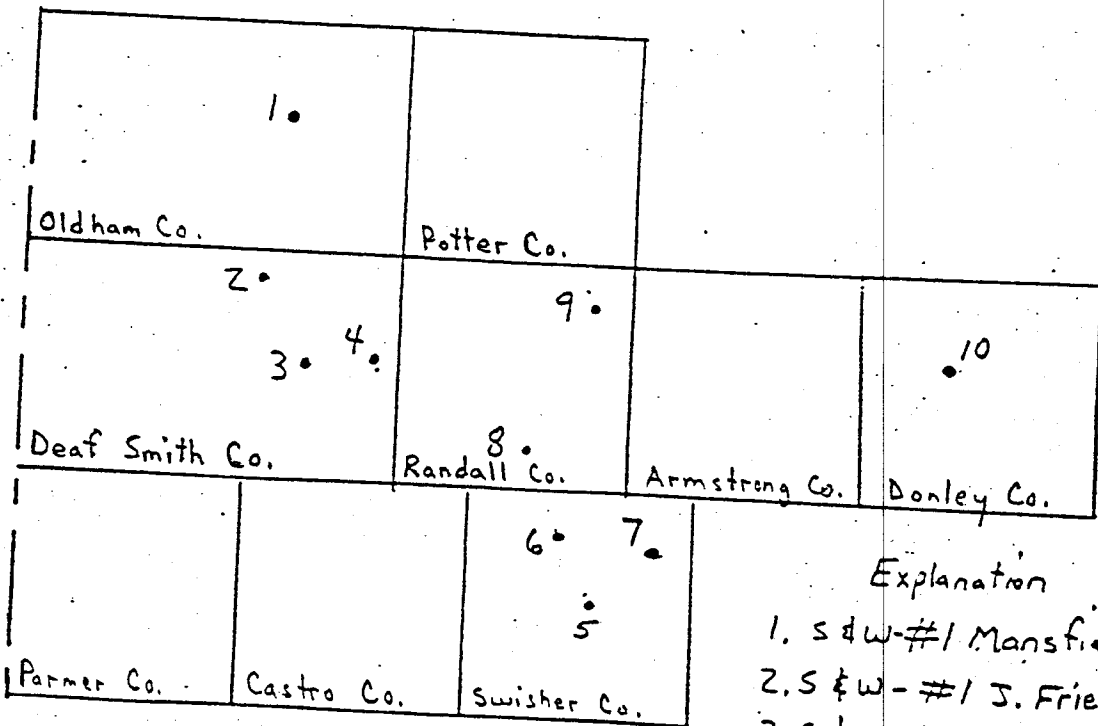
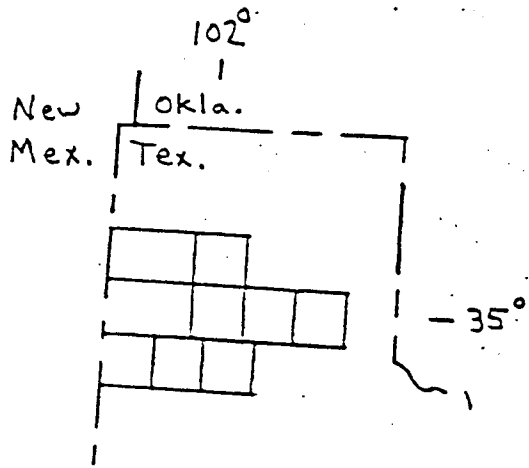


Fig. 10

SUPERSEDED

DRAFT



Explanation

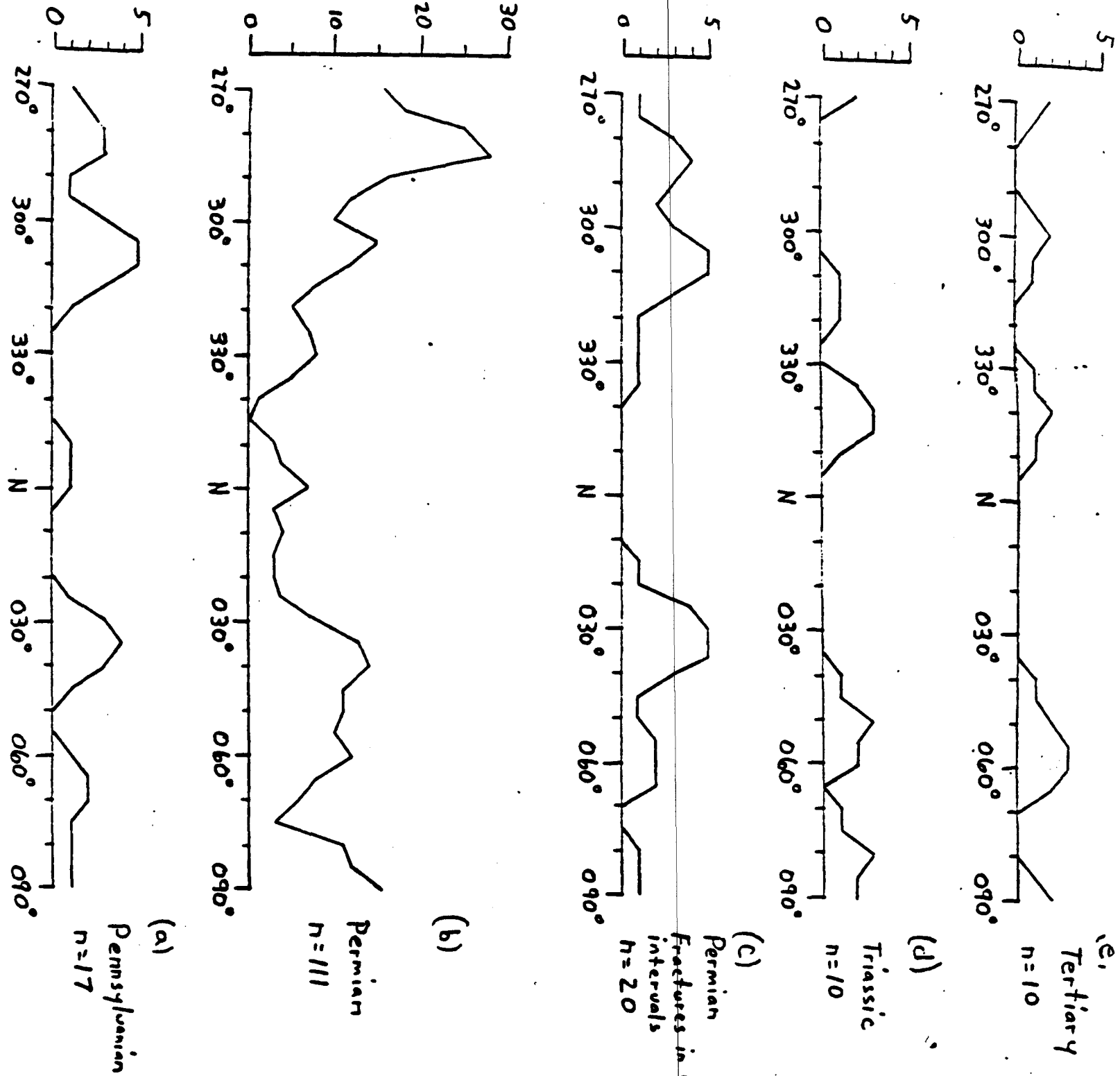
- 1. S & W - #1 Mansfield
- 2. S & W - #1 J. Friemel
- 3. S & W - #1 Deffen
- 4. S & W - #1 G. Friemel
- 5. S & W - #1 Zeeck
- 6. S & W - #1 Harman
- 7. Gruy-Federal - #1 Grabbe
- 8. S & W - #1 Holtzclaw
- 9. Gruy-Federal - #1 Rex White
- 10. Gruy-Federal - #1 Sawyer

**SUPERSEDED**

**DRAFT**

Fig. 11

Number of Measurements across 10° Increments

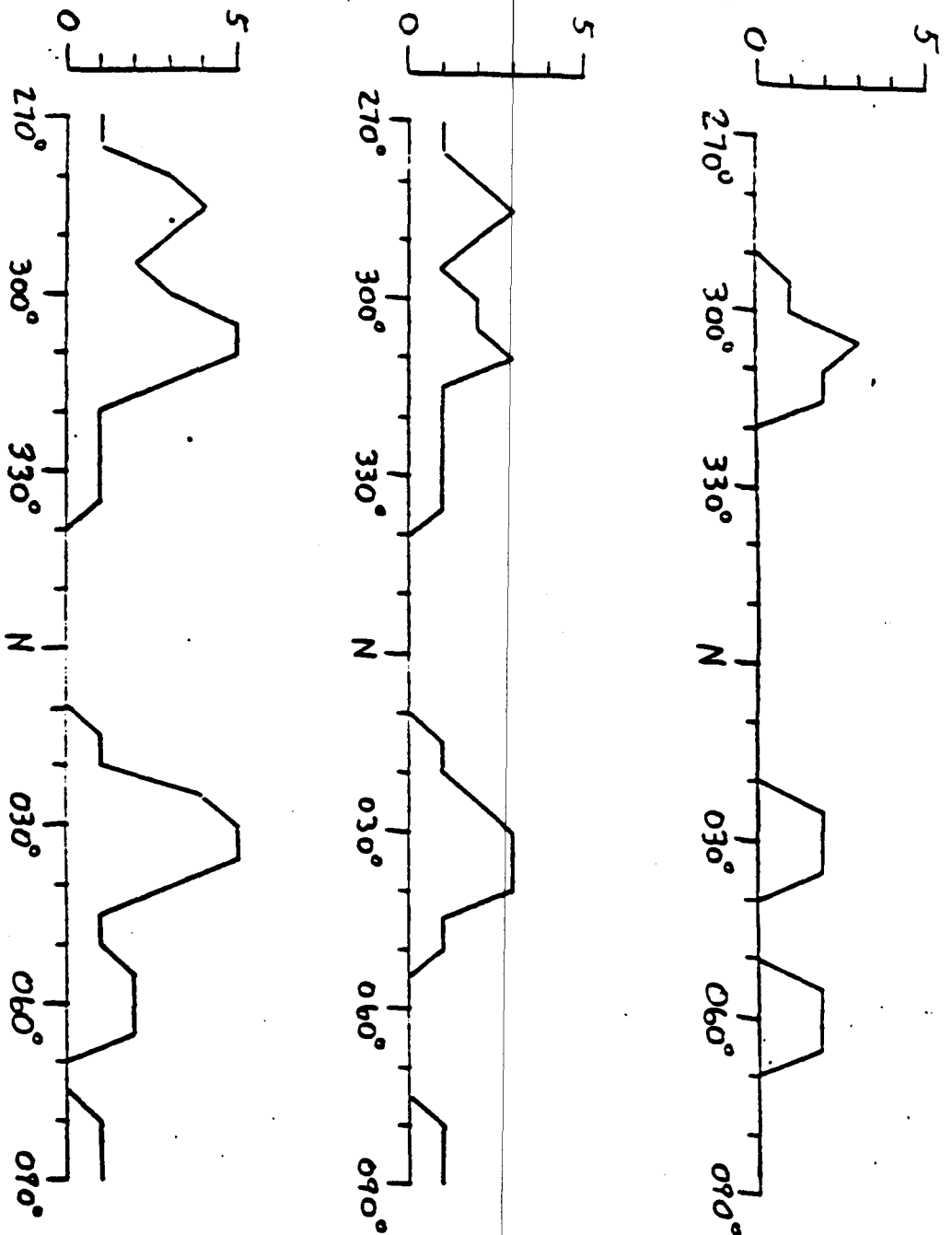


SUPERSEDED

Fig. 12

DRAFT

Number of Measurements across 10° Increments



(a)  
Permian  
Fractures in cored  
intervals  
n = 20

(b)  
Vein-filled fractures

(c)  
Fractures not  
vein-filled

SUPERSEDED

DRA

Number of Measurements across 10° Increments

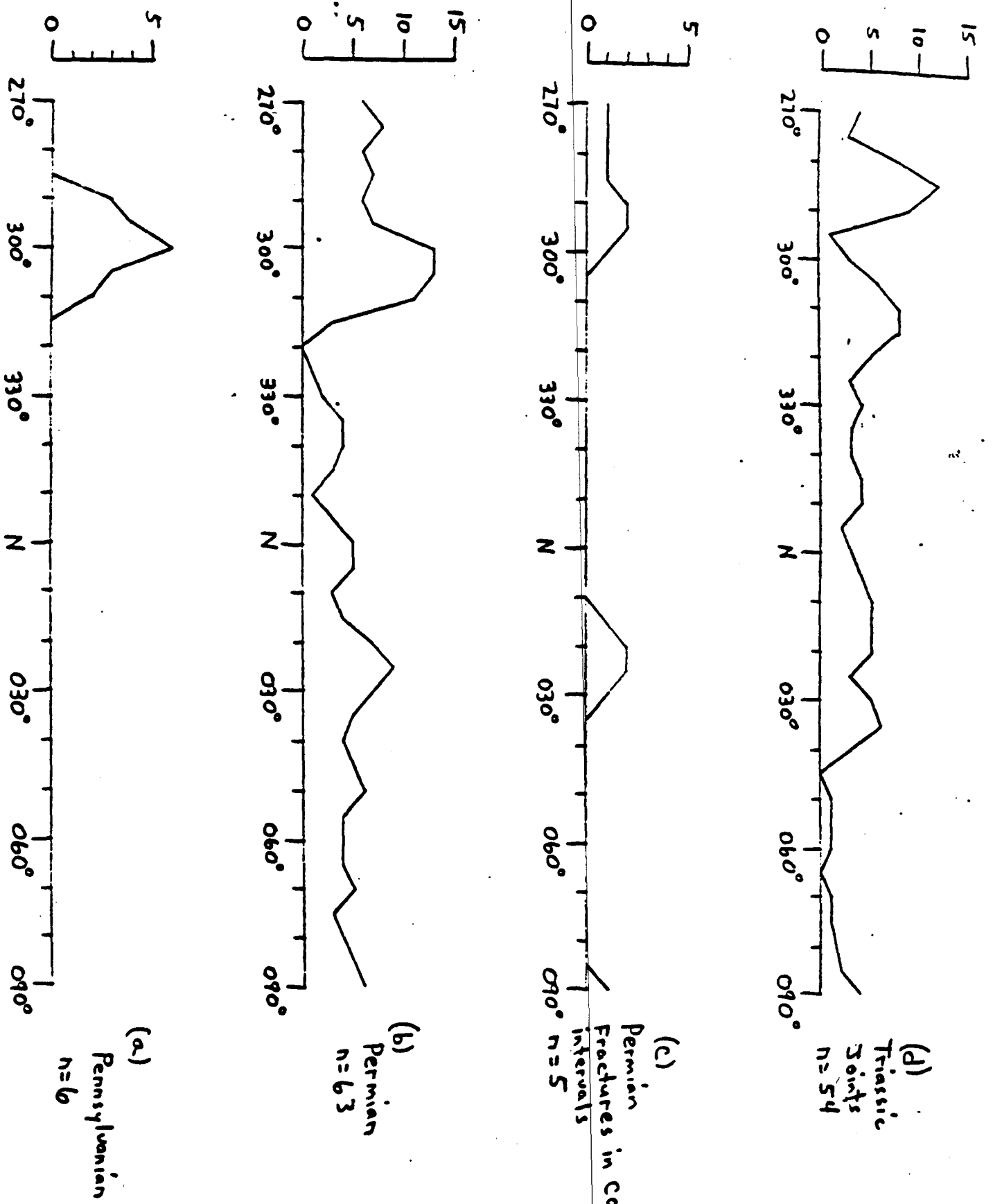


Fig. 14

**SUPERSEDED**

**DRAFT**

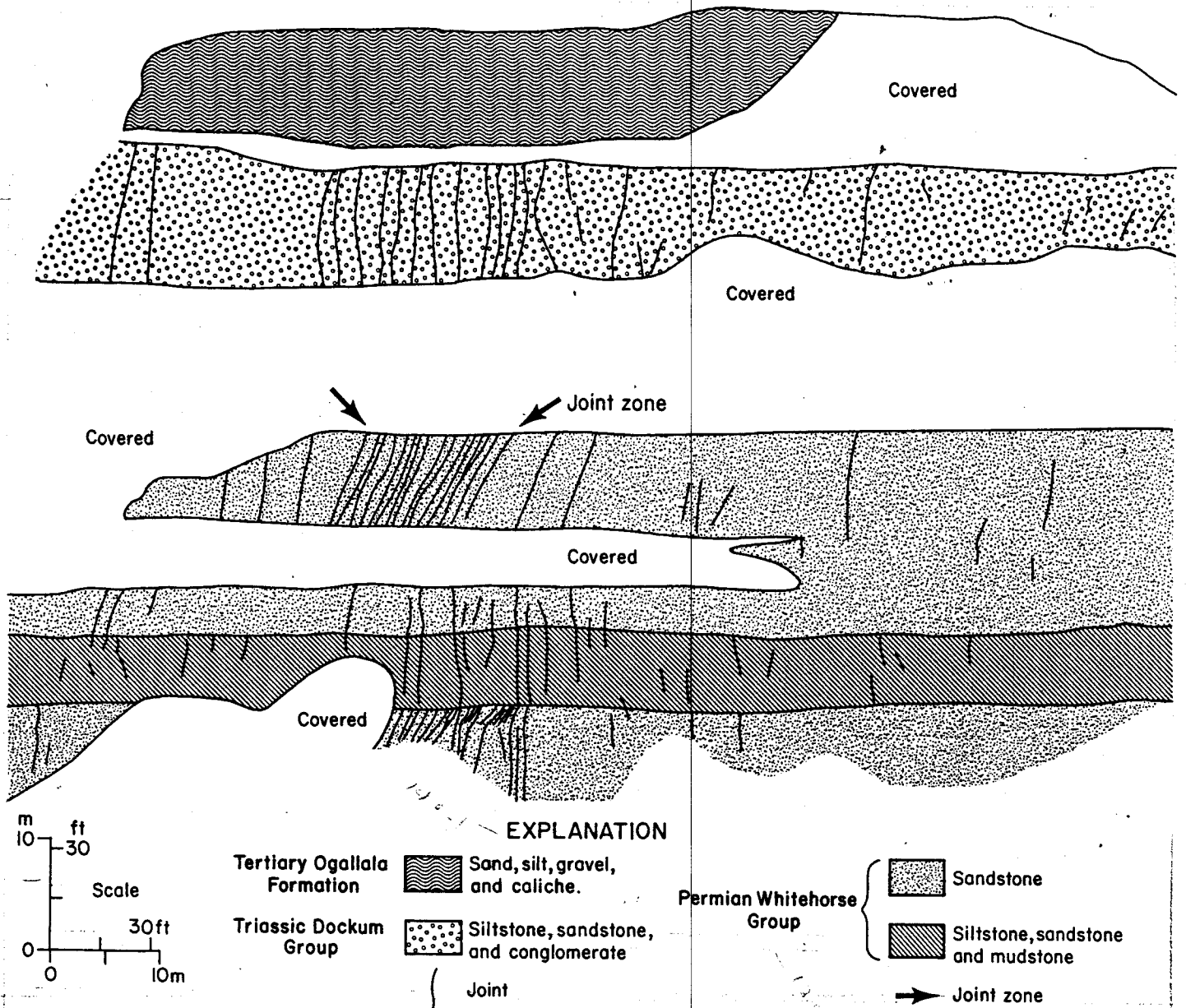


Fig. 15

**SUPERSEDED**

**DRAFT**

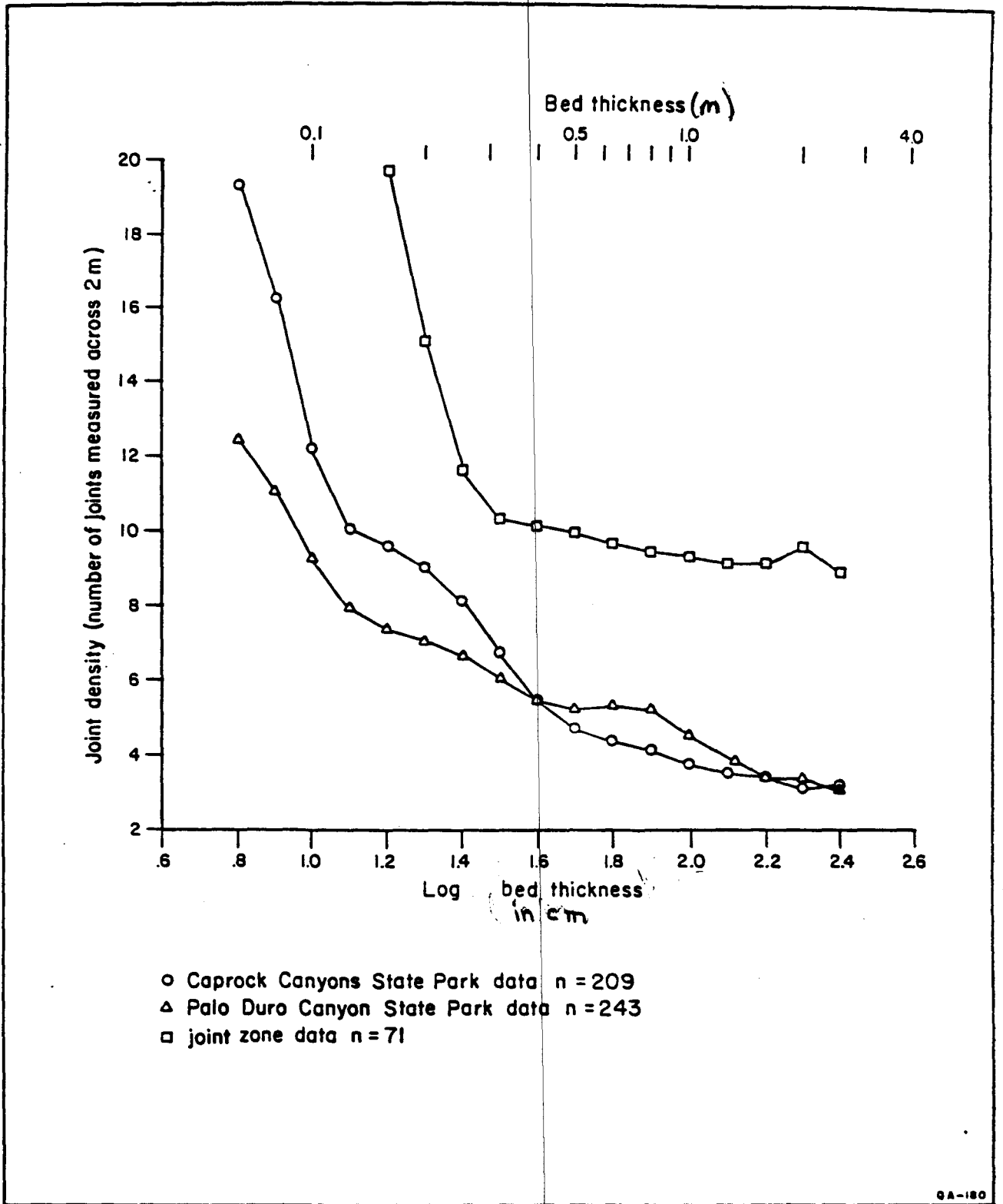


Fig. 16

SUPERSTAMP

TITLE	Graph - joint Density across 2 m vs bed thickness WTCU1 Circ.	DRAWING CONTROL NUMBER:	180
AUTHOR	E. Collins	DATE	11-18-82
DESIGNER	R. Platt		
REVISIONS	DJR.		

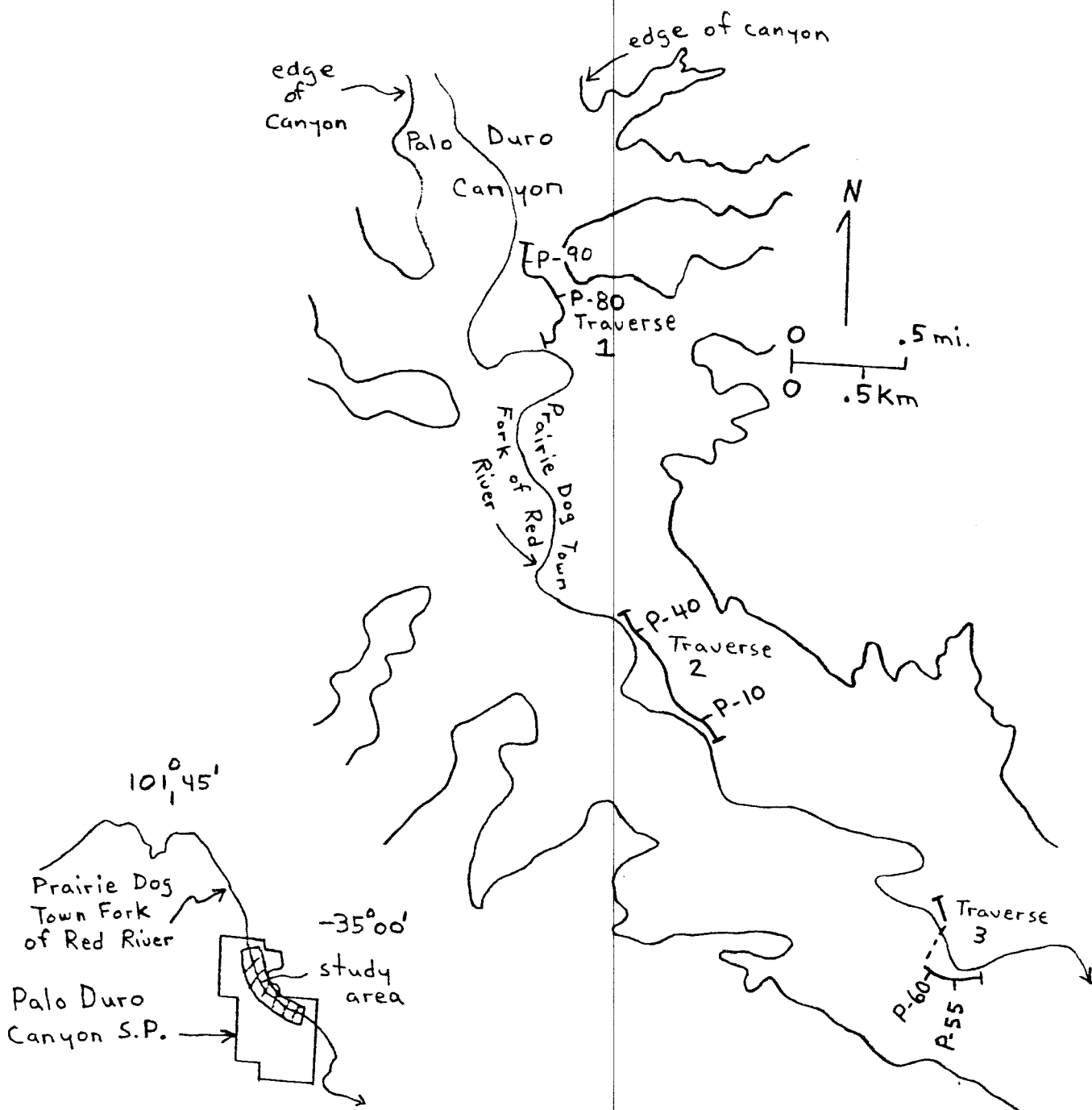
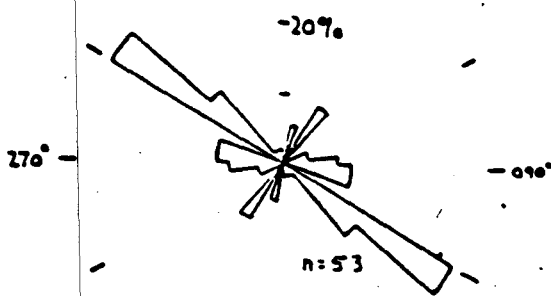
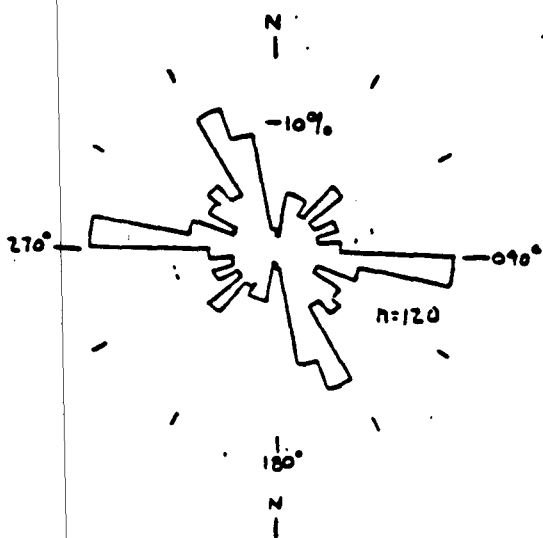
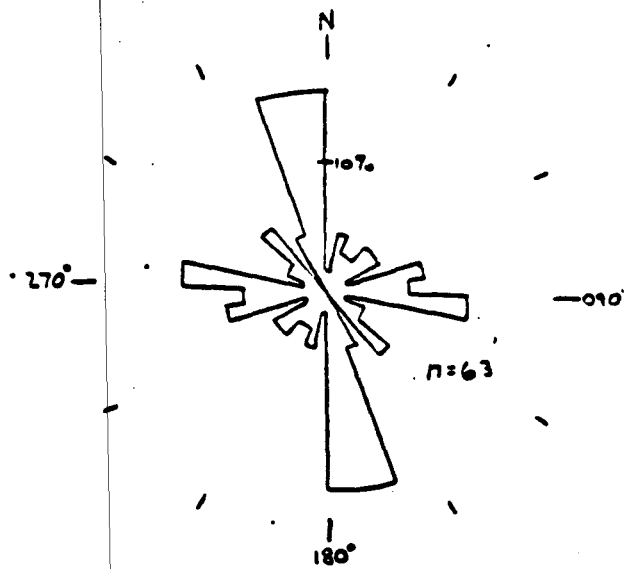
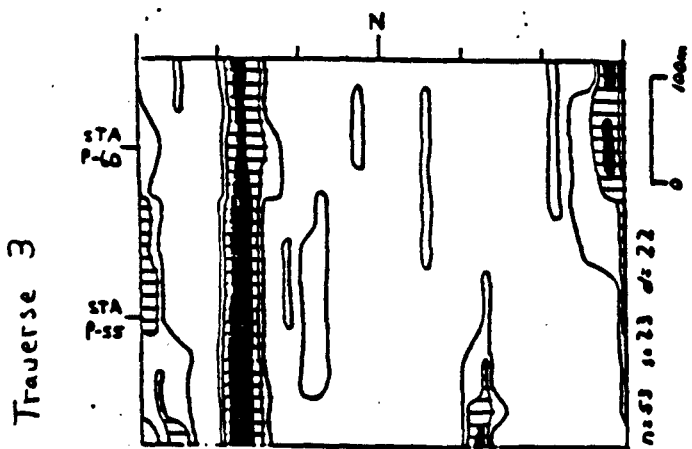
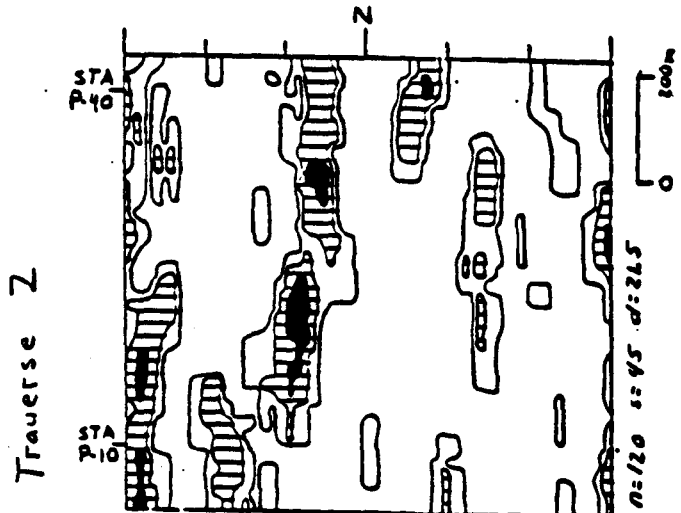
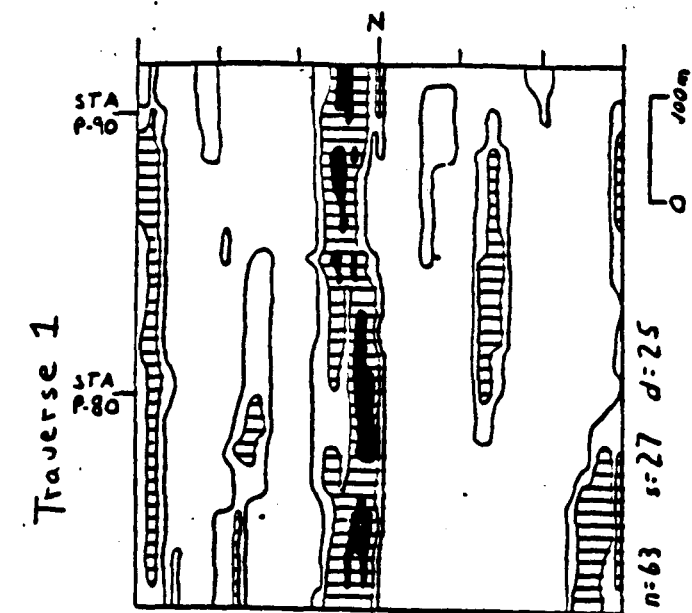


Fig. 17

**SUPERSEDED**

**DRAFT**



**SUPERIMPOSED**

FIG. 18

**DRAFT**

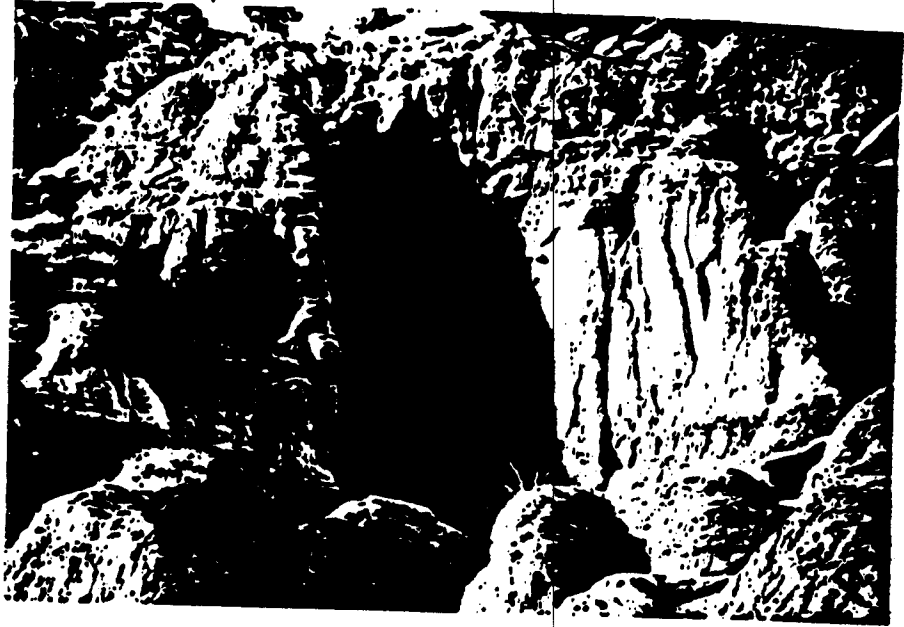


Fig. 19.

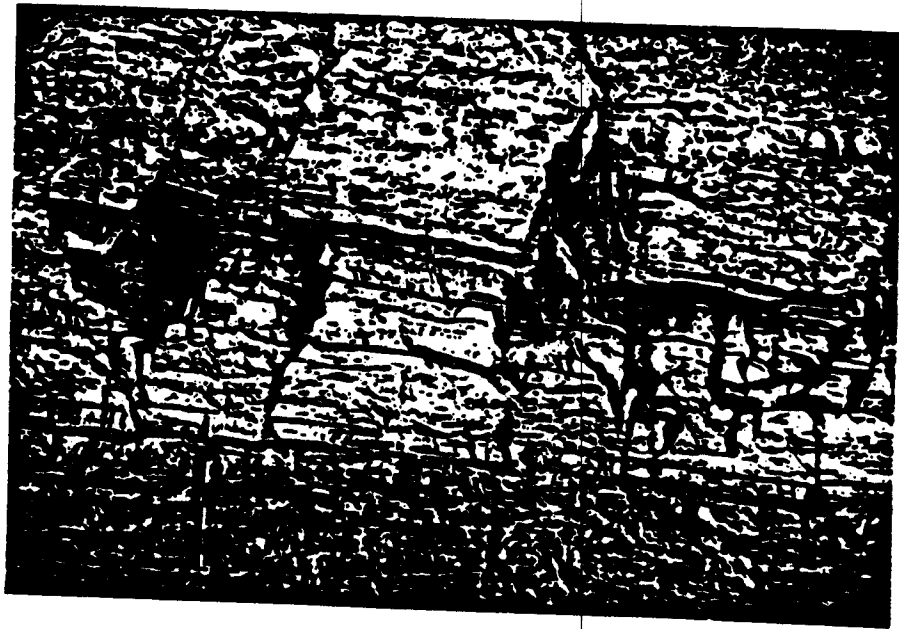


Fig. 20.

**SUPERSEDED**

**DRAFT**

SUPERSEDED  
DRAFT

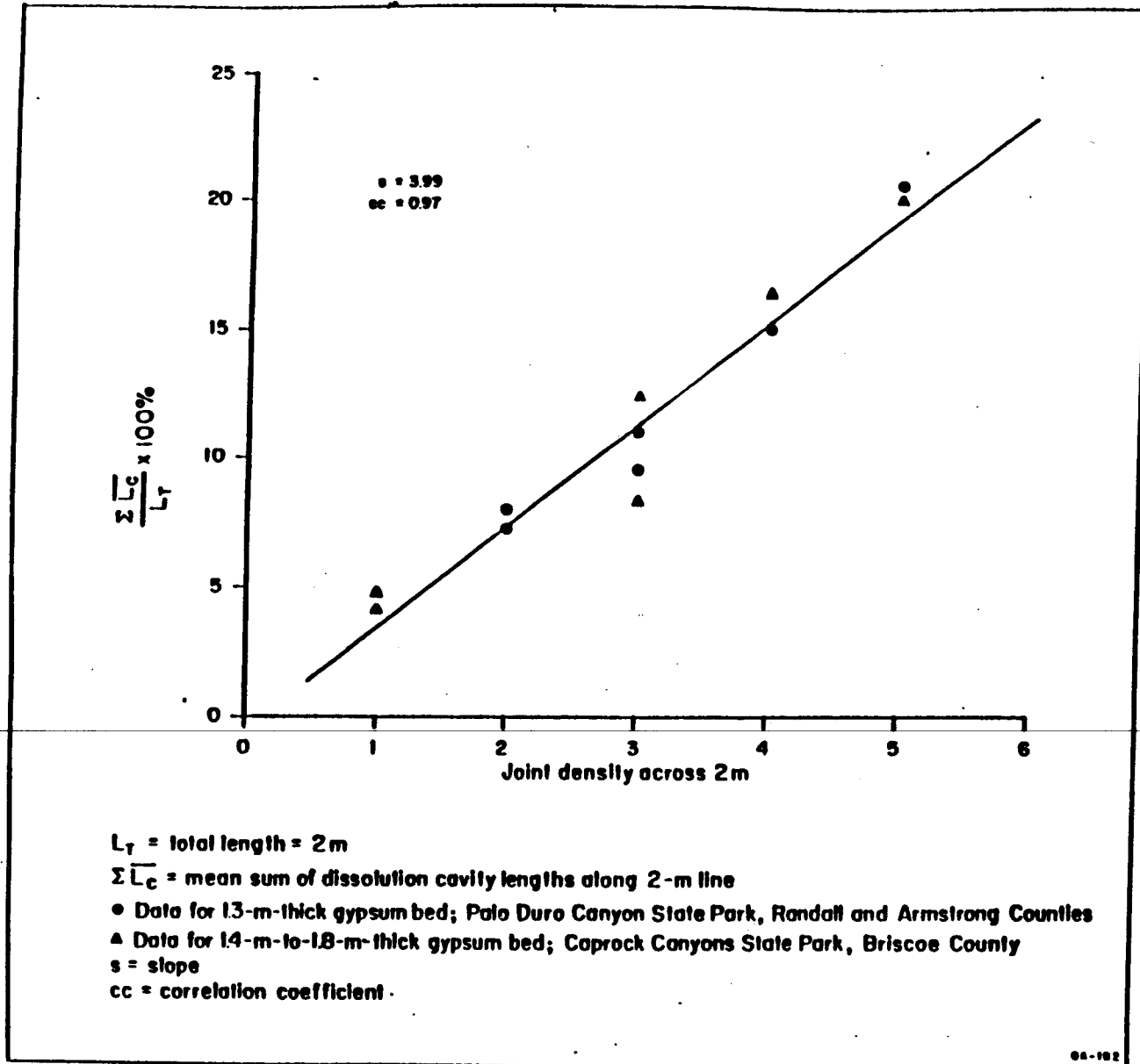
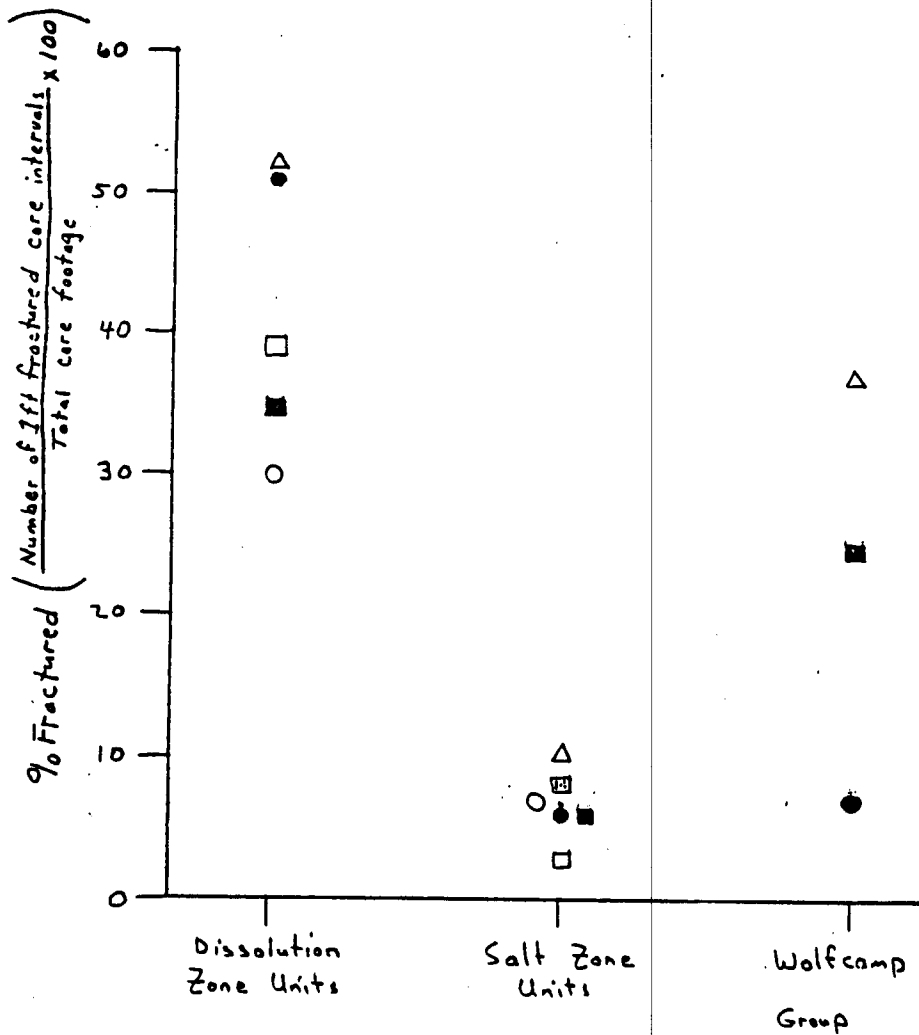


Fig. 21



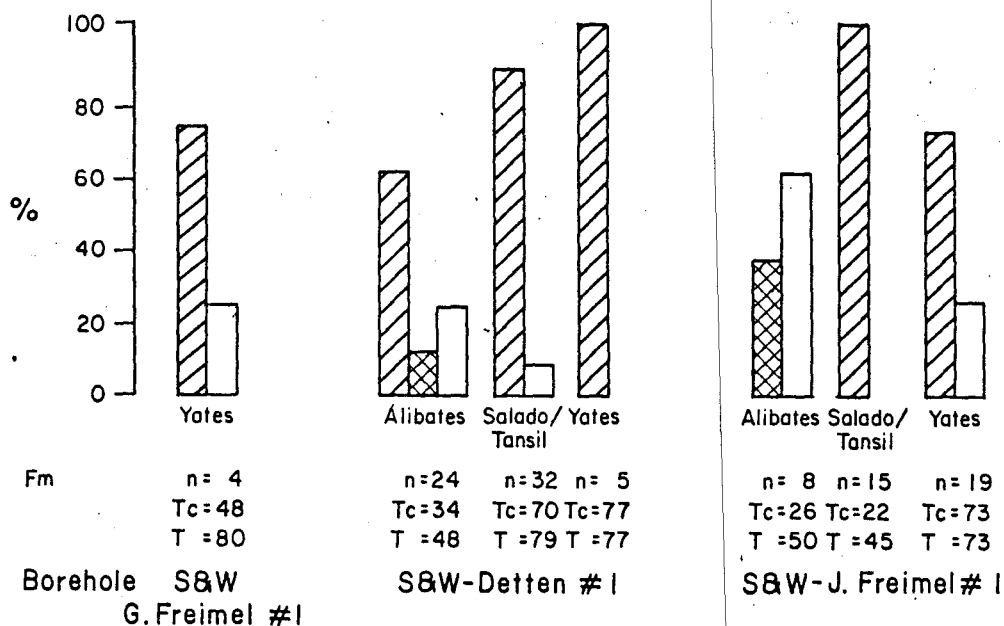
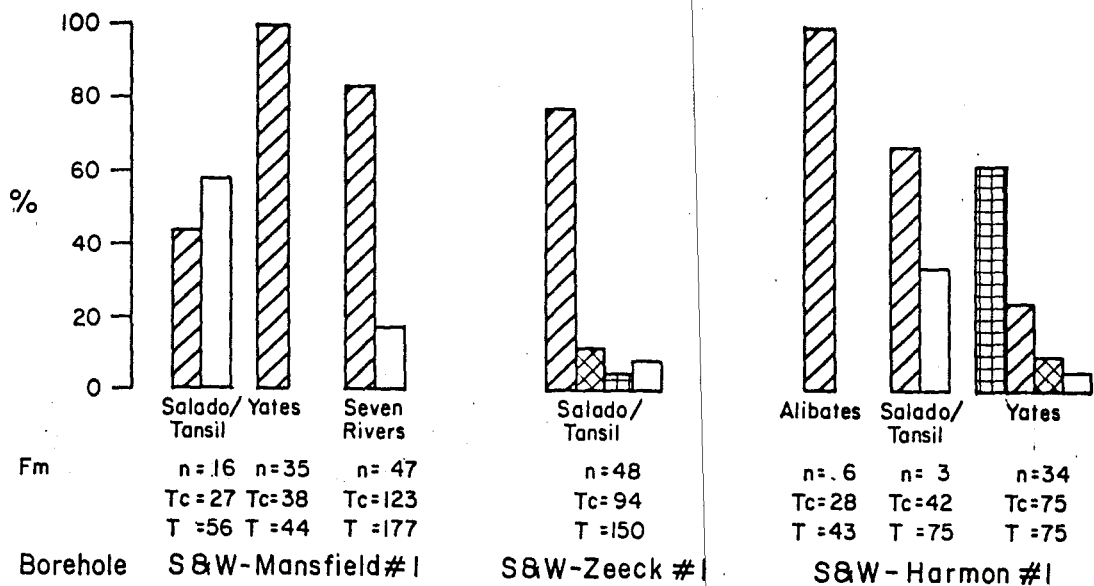
EXPLANATION

Well	Dissolution Zone Units	Salt Zone Units
▲ S&W-Mansfield #1	A, S/T, Y, SR	QG, SA, G, uCF, T, ICF
◆ S&W-S. Freimel #1	A, S/T, Y, SR	SR, SA
□ S&W-Detten #1	A, S/T, Y	SA
▣ S&W-G. Freimel #1		SR, QG, SA
● S&W-Zeeck #1	S/T	SA
○ S&W-Harmon #1	A, S/T, Y	QG, SA

SUPERSEDED  
COPIED FOR OFFICE

Fig. 22

**DRAFT**



EXPLANATION

- % Gypsum - filled fractures
- % Anhydrite - filled fractures
- % Halite - filled fractures
- % Fractures with no vein filling described

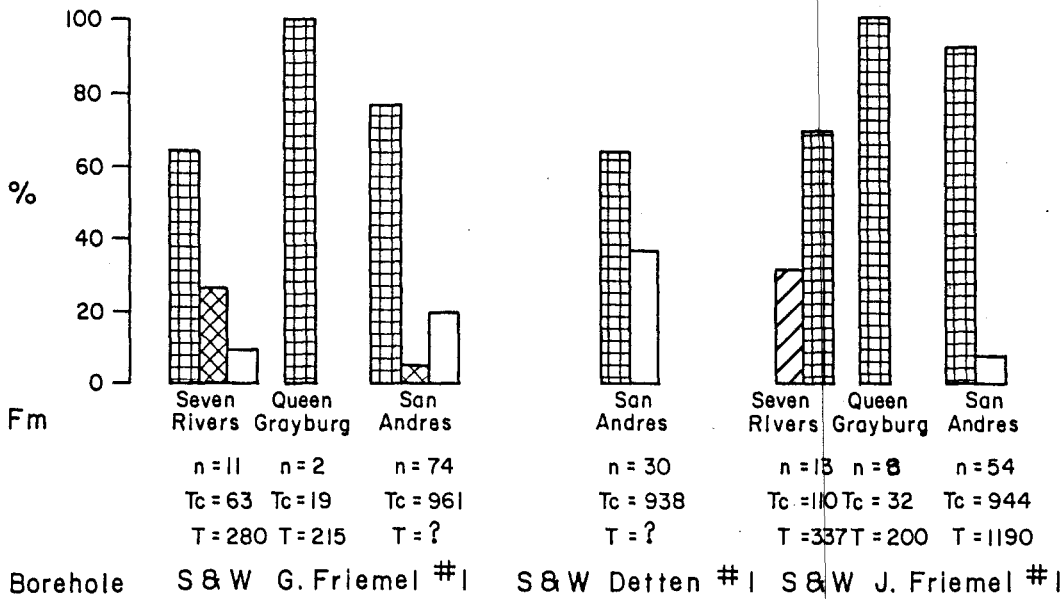
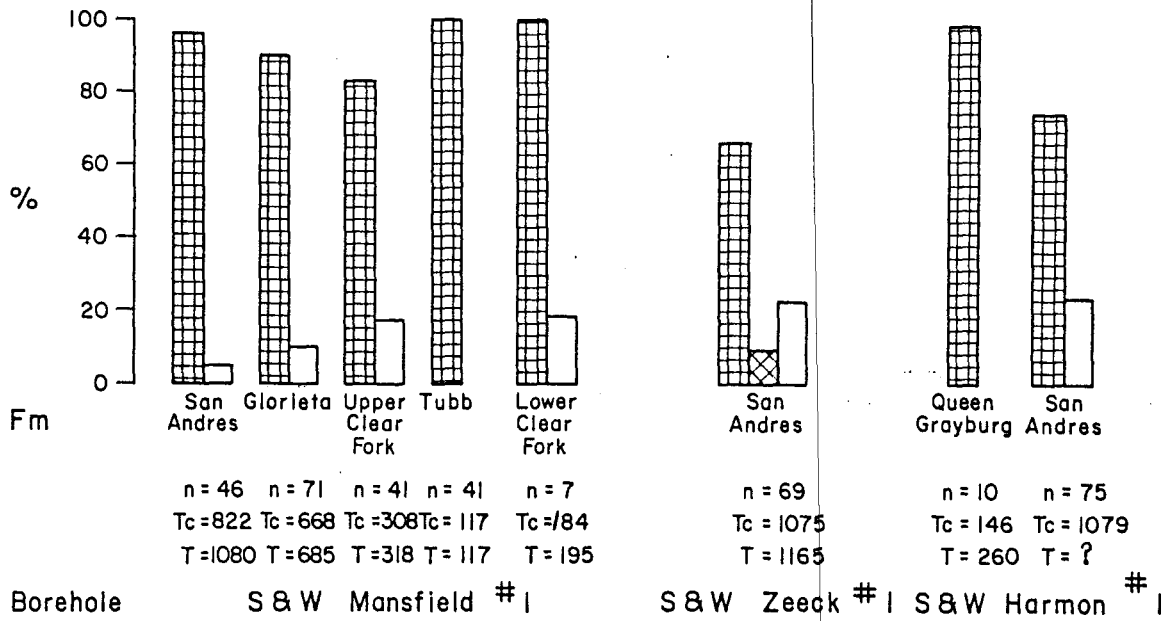
n = Number of one foot core increments with fractures  
 Tc = Total thickness of recovered core (feet)  
 T = Thickness of unit (feet)

QA 4502

**DRAFT**

**SUPERSEDED**

Fig. 23



 % Halite filled fractures  
 % Anhydrite filled fractures  
 % Fractures with no vein filling described  
 % Gypsum filled fractures

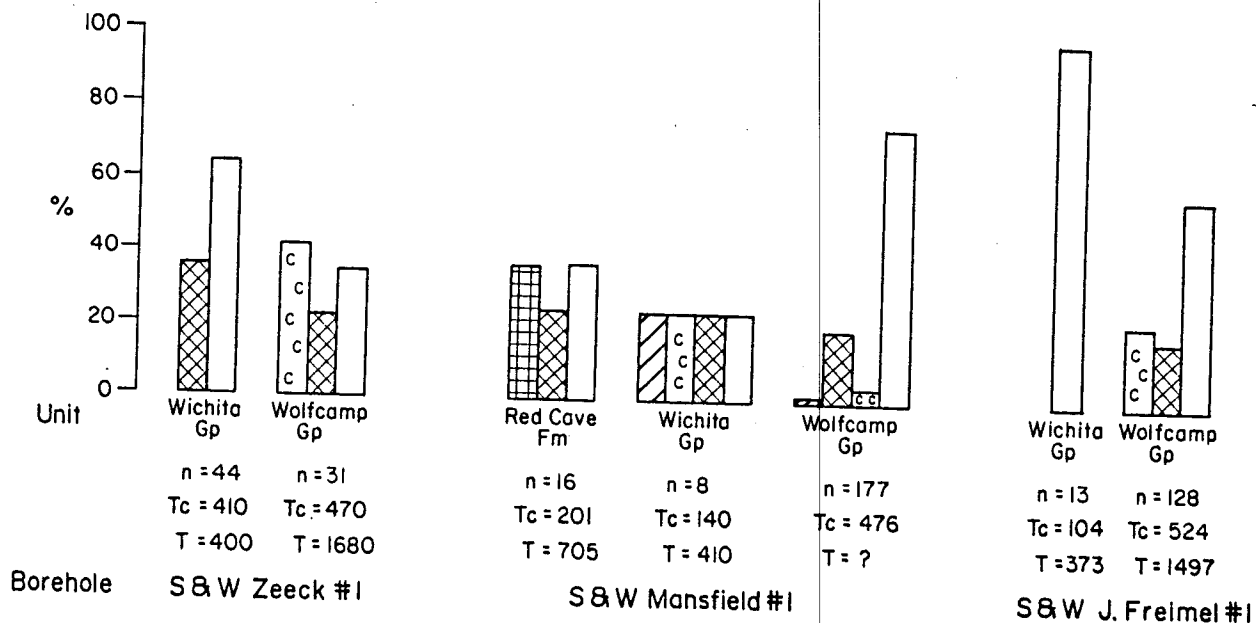
n = Number of one foot core increments with fractures  
 Tc = Total thickness of recovered core (feet)  
 T = Thickness of unit (feet)  
 T = ? Borehole not drilled to base of unit

QA4503

Fig. 24

**SUPERSEDED**

**DRAFT**



EXPLANATION

-  % Anhydrite filled fractures
-  % Gypsum filled fractures
-  % Halite filled fractures
-  % Calcite filled fractures
-  % Fractures with no vein filling described

- n = Number of one foot core increments with fractures
- Tc = Total thickness of recovered core (feet)
- T = Thickness of unit (feet)
- T = ? Borehole not drilled to base of unit

QA 4504

Fig. 25

**SUPERSEDED**

**DRAFT**



fig. 27

DOE-GRUY FEDERAL  
#1 REX WHITE



532 ft.



fig. 26

**SUPERSEDED**

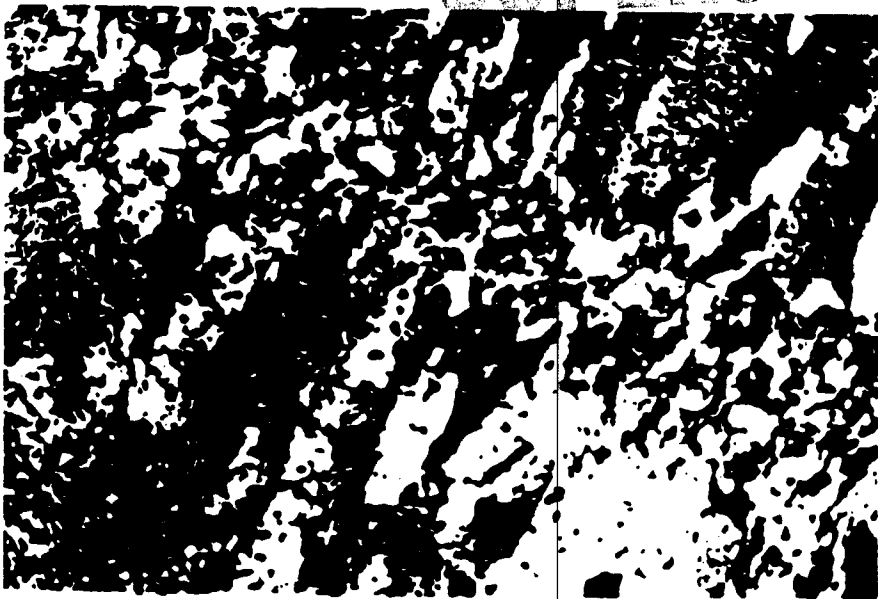


fig. 28

**DRAFT**



figure 29



figure 30

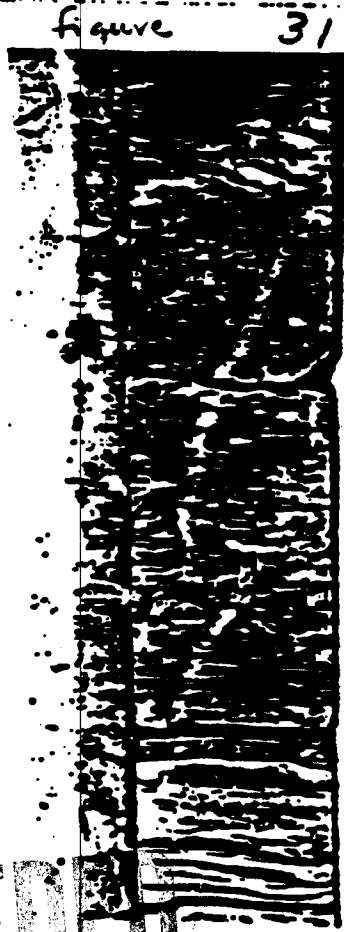


figure 31

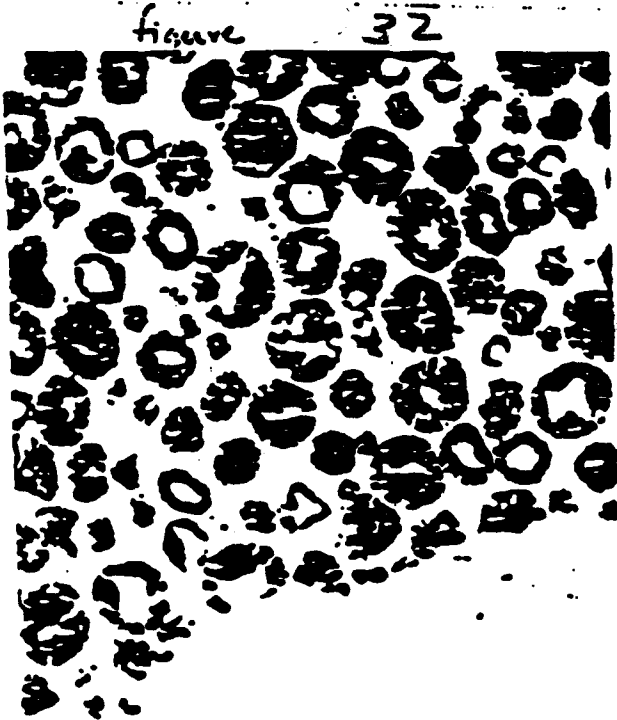


figure 32

DOE-STONE & WEBSTER  
#1 MANSFIELD

0 — — — — — 10 cm  
1992.5 - 1994.11.

SUPERSEAL

DRAFT



Figure

33

SUPERSEDED

**DRAFT**

DRAFT

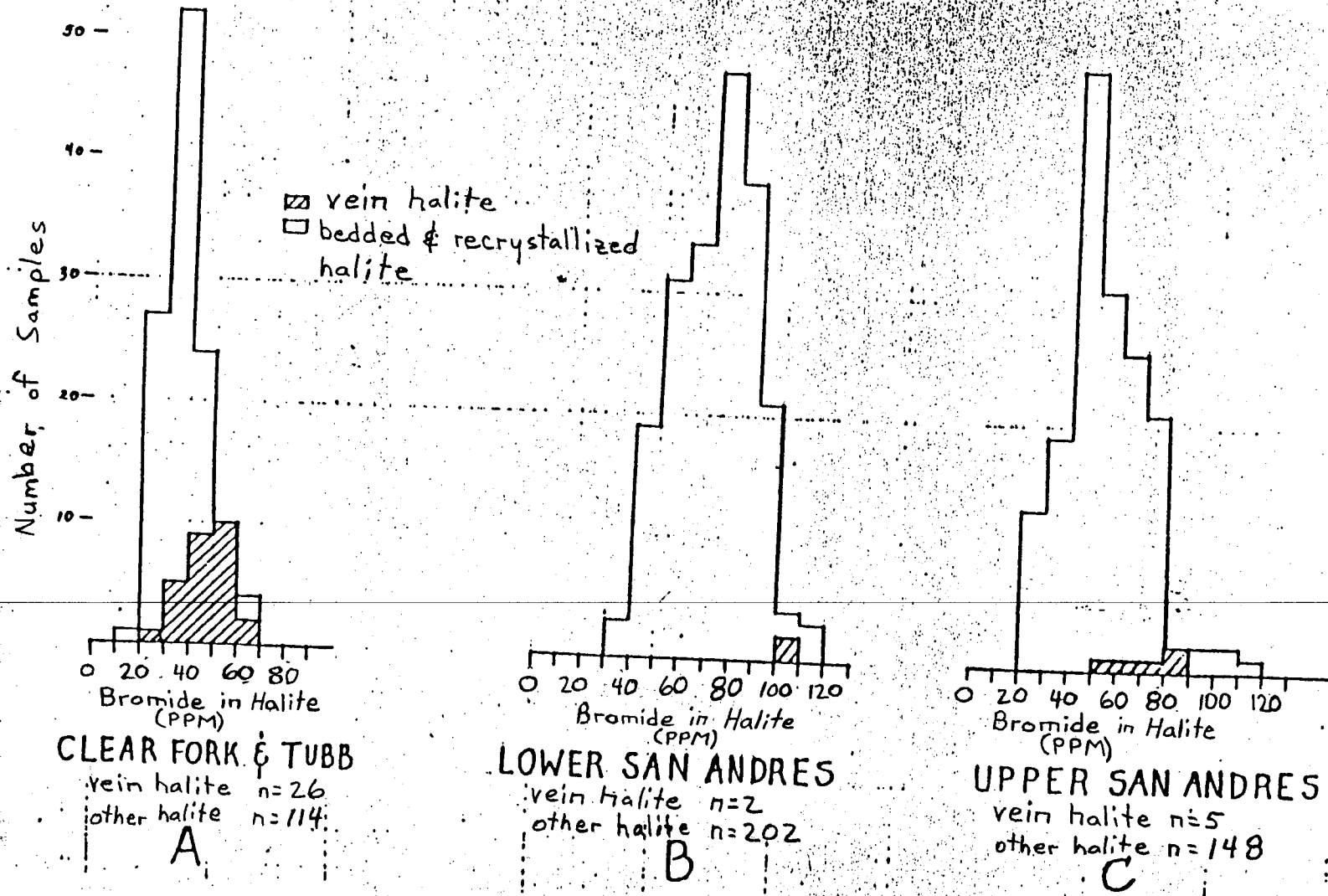


Figure 34